Journal of Wind Engineering
and Industrial Aerodynamics 96 (2008) 1498–1527

JOURNAL OF wind engineering AND industrial aerodynamics

www.elsevier.com/locate/jweia

# Prediction of wind environment and thermal comfort at pedestrian level in urban area

Akashi Mochida*, Isaac Y.F. Lun

*Tohoku University, 6-6-11-1202 Aoba, Aramaki Aza, Aoba-ku, Sendai, Japan*

Available online 15 April 2008

**Abstract**

This paper reviews the recent developments in CWE research for predicting the pedestrian level wind and thermal environments in urban areas, primarily achieved by the researchers in the field of environmental engineering in Japan. First the progress in turbulence models in the last decade and in their applications to the problems related to wind climate is briefly reviewed, and the results of Architectural Institute of Japan (AIJ) collaborative project in cross comparisons of CFD results of wind environments are presented. Next, recent achievements in the field of modeling canopy flows for reproducing the aerodynamic and thermal effects of trees, buildings and automobiles are outlined. Examples of numerical results obtained using tree and vehicle canopy models are shown to demonstrate the significant effects of stationary and non-stationary subgrid scale flow obstacles on turbulent flowfield within street canyons.


*Keywords:* Pedestrian level wind environment; Thermal comfort; Urban Heat Islands; Subgrid scale flow obstacles; Tree canopy; Vehicle canopy

## 1. Introduction

The world's urban population was 2.9 billion (47.2%) in 2000 and is expected to rise to 5 billion (60.2%) by 2030. During 2000–2030, the world's urban population is projected to grow at an average annual rate of 1.9% (World Urbanization Prospects, 2001). In line with the rapid urbanization and growth of urban population, there are increasing concerns

*Corresponding author. Tel.: +81 22 795 7884; fax: +81 22 795 7886.
*E-mail address:* mochida@sabine.pln.archi.tohoku.ac.jp (A. Mochida).

0167-6105/$ - see front matter 
doi:10.1016/j.jweia.2008.02.033

regarding the quality of urban environment. In this respect, urban thermal environment is one of the major concerns, which had lead to numerous researches on this topic. The urban thermal environment has been worsened by the Urban Heat Island (UHI) effects. The UHI is now regarded as one of the most serious urban environmental problems in the world. The contributing factors of UHI include less vegetation in city area, absorption of solar energy input by concrete and paved surfaces, multiple heat reflections from canyon structures of high-rise buildings, anthropogenic heat releases from air-conditioning systems, automobiles, etc. In order to reduce the UHI effects, various mitigating measures have been proposed. The most commonly applied is tree planting. The monetary benefits of urban trees are difficult to quantify because these trees can provide numerous private and public benefits. The latter includes improving thermal environment, reducing air pollution and community noise problems, enhancing biodiversity and meliorating aesthetics (Akabari et al., 1992; McPherson and Rowntree, 1993; Rowntree, 1989). Thus, the existence of tree covered ground surface is one of the most essential factors to be considered in urban design. Accurate reproduction of aerodynamic effects of trees is also very significant for predicting wind environment in urban area.

Wind environment is one of the most important factors to be considered in UHI study as it has significant influence on UHI effect and outdoor thermal comfort. The conventional urban wind environment assessment methods only took into consideration the influence of topographic features and geometry of buildings (cf. Fig. 1(1)). These methods may be inadequate to reflect the real conditions of city where there are objects of

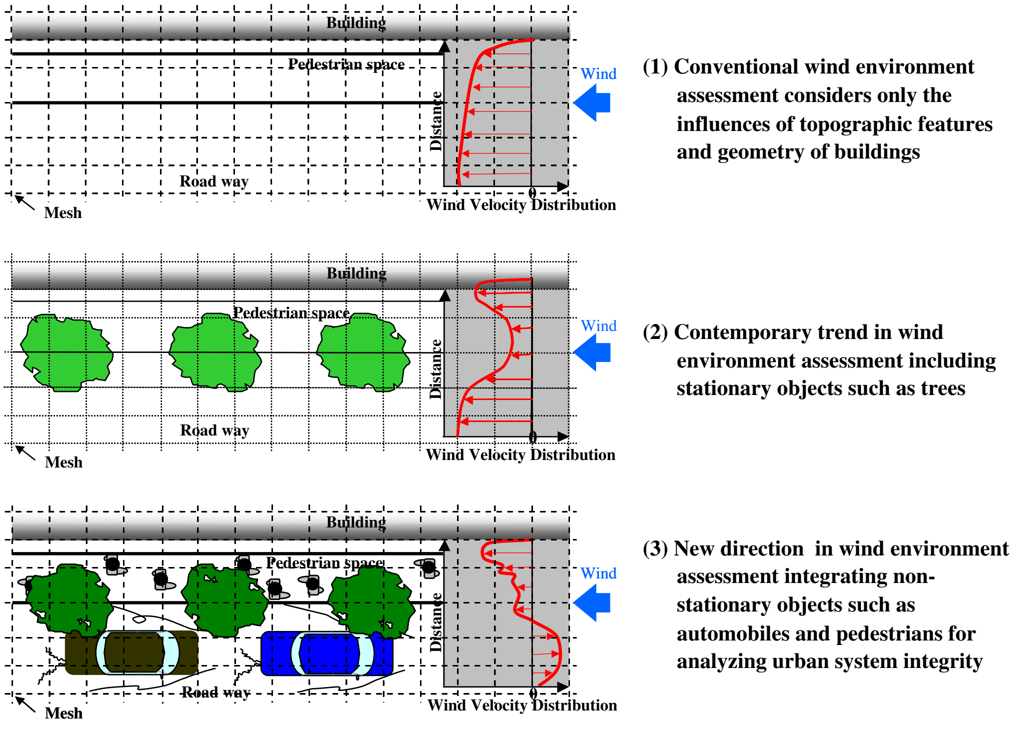


Fig. 1. Concept of wind environment assessment: from conventional approach to contemporary tactics.

various scales within the street canyons. Stationary objects (cf. Fig. 1(2)) such as trees and telephone boxes, and non-stationary objects (cf. Fig. 1(3)) such as moving vehicles and swinging hanging-signboards (commonly seen in Asian countries), may alter the surface roughness to certain extent. In order to obtain accurate quantitative data for urban wind environment assessment, these objects must not be overlooked. In recent years, canopy models for reproducing the aerodynamic and thermal effects of trees, buildings and automobiles have been developed and applied to various problems related to urban climate. The canopy models were incorporated into the meteorological mesoscale models. The simulation methods for mesoscale and microscale climates were then integrated into the total simulation system using the nested grid technique.

The growth of CWE applications in the past decade had greatly expanded the scope of wind engineering. Now the application of CWE ranges from the microclimate around a human body to the mesoscale climate in urban area. The aims of this paper are to present the progress of CWE researches for predicting pedestrian level wind environment around buildings primarily achieved by the researchers in the field of environmental engineering in Japan, together with a brief review on turbulence modeling for CWE applications to problems related to wind environment and cross comparison of predicted results with various turbulence models for several test cases, and to demonstrate the significant effects of stationary and non-stationary objects (tree canopy and vehicle canopy, respectively) on turbulent diffusion process within street canyons.

## 2. Progress in turbulence modeling for CWE applications over the past 10 years

### 2.1. Appearance of dynamic SGS models and their applications in wind engineering

The standard Smagorinsky model was widely used in the computation of LES in the CWE researches conducted in the early period. In the Smagorinsky model approach, a simple eddy-viscosity type approximation is used to simulate the subgrid scale (SGS) stress $\tau_{ij}$ in SGS. The SGS eddy viscosity, $\nu_{\mathrm{SGS}}$, is estimated by

$$\nu_{\mathrm{SGS}} = (C_S f_\mu \bar{\Delta})^2 \cdot \sqrt{\frac{1}{2}\left(\frac{\partial \bar{u}_i}{\partial x_j} + \frac{\partial \bar{u}_j}{\partial x_i}\right)^2} = C(f_\mu \bar{\Delta})^2 \sqrt{\frac{1}{2}\left(\frac{\partial \bar{u}_i}{\partial x_j} + \frac{\partial \bar{u}_j}{\partial x_i}\right)^2} = C(f_\mu \bar{\Delta})^2 |\bar{S}|, \tag{1}$$

where $\bar{f}$ is the filtered quantities, $\bar{\Delta}$ the grid-filter width, $f_\mu$ the wall damping function.

In the standard Smagorinsky model, one value of the Smagorinsky constant, $C_{\mathrm{S}}$, must be selected. The Smagorinsky constant $C_{\mathrm{S}}$ was optimized from 0.1 to 0.25 for various flowfields. Since the flowfield around a bluff body involves various types of flow properties such as impingement, separation, free shear layer, vortex shedding, etc., it is arduous to determine an appropriate value of $C_{\mathrm{S}}$ for analyzing the whole flowfield around the bluff body. The dynamic SGS model, which was proposed by Germano et al. (1991) and revised by Lilly (1992), successfully corrected this fault of the standard Smagorinsky model. In the dynamic SGS model, based on the Smagorinsky model (hereafter denoted by DS model), the value of model coefficient $C\ (=C_{\mathrm{S}}^2)$ was determined as a variable quantity depending on space and time, and following the properties of the flowfield. Two filters with different characteristic scales, i.e. grid filter and test filter (Germano et al., 1991), were used in this approach. The details of this model are available in many papers (Lilly, 1992; Ferziger, 1996; Voke, 1996; Rodi et al., 1997; Murakami et al., 1996a, b; Murakami and Mochida, 1999).

It was affirmed in the 1990s that the prediction accuracy of the static type Smagorinsky model could be improved by the DS model (Voke, 1996; Rodi et al., 1997; Murakami et al., 1996a). However, computation based on the DS model was not stable as the fluctuation of $C$ was too large. In order to stabilize the fluctuation of $C$, various techniques and models had later been proposed (Zang et al., 1993; Vreman et al., 1994; Meneveau et al., 1996; Murakami et al., 1996b, 1999; Murakami and Mochida, 1999; Tominaga et al., 1997). When the flowfield has a homogeneous direction (e.g. channel flow), $C$ can be calculated using the averaged quantity of the homogeneous direction. However, this technique cannot be used in many problems in wind engineering which deals with three-dimensional (3D) flow around a bluff body. To deal with such 3D flow, the Lagrangian dynamic model proposed by Meneveau et al. (1996) is useful. In this model, $C$ is calculated using the averaged quantities along the flow path line instead of using quantities averaged over the homogeneous direction. Murakami et al. (1999) applied this model to flow past a square cylinder and found that this model remarkably improved both the calculation stability and prediction accuracy when a proper length scale was imposed on Lagrangian averaging.

It is widely known that the DS model requires the principal axes of the SGS stress term $\tau_{ij}$ be aligned with the strain-rate tensor and this brings about an excessive energy back-scattering when $C$ becomes negative. In order to overcome this shortcoming, the dynamic mixed model (hereafter denoted by DM model) was proposed by Zang et al. (1993) and revised by Vreman et al. (1994), as a linear combination of the DS model and the scale-similarity model (Bardina et al., 1981), to control the extent of excessive back-scattering. The basic equations of DM model are

$$\begin{aligned}\tau_{ij} - \frac{1}{3}\delta_{ij}\tau_{kk} &= \underbrace{-2\nu_{\mathrm{SGS}}\bar{S}_{ij}}_{\text{Smagorinsky model}} + \underbrace{B_{ij} - \tfrac{1}{3}\delta_{ij}B_{kk}}_{\text{scale-similarity model}} \\ &= -2C\bar{\Delta}^2|\bar{S}|S_{ij} + B_{ij} - \frac{1}{3}\delta_{ij}B_{kk},\end{aligned} \tag{2}$$

$$B_{ij} = \overline{\bar{u}_i\bar{u}_j} - \bar{\bar{u}}_i\bar{\bar{u}}_j, \tag{3}$$

where $C$ is given by utilizing the dynamic procedure (Lilly, 1992). Tominaga et al. (1997) applied the DM model to simulate the flow past a bluff body and gas diffusion around a building. It was confirmed that this model yielded better results than the DS model.

Recently, Iizuka and Kondo (2004) studied the flow over a 2D hill using the DS model. In their results, the DS model showed very poor agreement with the experiment results. It was mainly due to the poor prediction accuracy in region near the ground surface. In order to overcome this drawback, they proposed a hybrid SGS model, i.e. a combination of static and dynamic types of the Smagorinsky model. Iizuka et al. also pointed out that the DM model significantly under-predicts the mean velocity values in the central region of channel flow. Inagaki et al. (2005) developed a new static type of the SGS model based on the "mixed time-scale" concept proposed by Abe et al. (1995). The performance of this model was examined for flow over a 2D hill by Iizuka and Kondo (2006).

### 2.2. Generation of inflow turbulence for LES

For the application of LES on a flowfield with obstacles, the technique for providing the inflow boundary condition is particularly important since the inflow condition adopted is always turbulent in wind engineering. In order to generate turbulent velocity fluctuations at the inflow boundary, several techniques have been developed (Lee et al., 1992; Kondo et al., 1997; Maruyama et al., 1997; Lund et al., 1998; Iizuka et al., 1999; Kataoka and Mizuno, 2002). The simplest method is to store the time history of velocity fluctuations given from a preliminary LES computation. Another approach is the artificial generation method in which velocity fluctuations are given by inversing the Fourier transform of prescribed energy spectrum with target turbulence intensity and length scale (Lee et al., 1992). Methods of generating the inflow turbulence for CWE applications based on this approach were developed by Kondo et al. (1997), Maruyama et al. (1997) and Iizuka et al. (1999). The third method is to set the driver section at the upstream region of the main computational domain to generate the inflow turbulence. Lund et al. (1998) proposed the method for generating 3D time-dependent turbulent inflow data for LES of spatially developing boundary layers. Kataoka and Mizuno (2002) simplified Lund's method by assuming the boundary layer thickness is constant within the driver section, and this method is now widely used in LES applications for wind engineering problems.

### 2.3. Applications of second-moment closure models in wind engineering problems

Algebraic Stress model (ASM) (Rodi, 1976) and Differential Second-moment Closure Model (DSM, or Reynolds Stress Equation Model (RSM)) (Launder et al., 1975) were applied to bluff bodies (Murakami et al., 1991, 1993). A number of DSMs were proposed during the early 1990s. The major topic was the revision of modeling for pressure–strain correlation term, including the higher-order models proposed by Fu–Launder–Tselepidakis (FLT model) (Fu et al., 1987) and Speziale–Sarkar–Gatski (SSG model) (Speziale et al., 1991). Concerning the wall reflection term, the present authors pointed out the shortcoming of the Gibson–Launder model (Gibson and Launder, 1978) when it was applied to bluff bodies. The stress normal to the wall should be suppressed in the impinging region while the Gibson–Launder model increases it (Murakami et al., 1991). Craft and Launder (1992) proposed a revised model in which this drawback was rectified.

Murakami et al. (1993) applied various DSMs to the flowfield around a cube. Their DSM results did not show any over-estimation of turbulent energy $k$ around the frontal corner, which is peculiar to the $k$–$\varepsilon$ model (Murakami et al., 1990). However, the lengths of separation region were over-estimated in all trials of DSM. LES based on the simple standard Smagorinsky model gave much better prediction, in comparison with DSM. Similar tendency of the drawbacks of DSM, when applied to flow around a cube, were also reported in the 6th ERCOFTAC/IAHR/COST workshop on the refined flow modeling (organized by Profs. Hanjalic and Obi, 1997).

### 2.4. Revisions of $k$–$\varepsilon$ models and their applications to wind engineering problems

It is widely recognized that the standard $k$–$\varepsilon$ model has a serious drawback in over-estimating turbulence kinetic energy, $k$, in the flow with impingement (Murakami et al., 1990). Although this problem does not occur in LES computations, the computational resource required for LES is large and is still beyond the scope of practical applications in CWE. Thus, $k$–$\varepsilon$ model is still favorable due to its simplicity and cost effectiveness (Wright and Easom, 1999; Wright et al., 2001). Several revised $k$–$\varepsilon$ models have been proposed to overcome the drawback of the standard $k$–$\varepsilon$ model and their performance have been tested for flow around a building, city block, actual building complex and flow over hilly terrains.

### 2.4.1. LK and MMK models

Launder and Kato (1993) proposed a revised $k$–$\varepsilon$ model (hereafter denoted by LK model) in which the production term $P_k$ in the transport equation of turbulent energy $k$ was changed from $P_k = \nu_t S^2$ to $P_k = \nu_t S\Omega$, as shown in Table 1 (in this paper, $\langle\ \rangle$ denotes ensemble-averaged quantities). They applied the LK model to a 2D oscillating square cylinder and obtained good results. With this revision, the over-estimation of $k$ around the frontal corner was remarkably improved while the increase in computer processing time (due to this modification) was very small. The LK model is very easily modified from the original standard $k$–$\varepsilon$ model and its computation stability is also very good in comparison to the non-linear $k$–$\varepsilon$ models (Speziale, 1987; Shih et al., 1993; Craft et al., 1995). Thus, the LK model is often applied to the flowfield around a bluff body (Lakehal and Rodi, 1997; Rodi, 1997). However, this model has two faults requiring revision. First, the LK model contributes to a decrease in turbulent energy $k$ at the area where $\Omega < S$, as shown in its definitions (cf. Eq. (7) in Table 1). However, it over-estimates the value of $P_k$ in comparison to the standard $k$–$\varepsilon$ model where $\Omega > S$. The area with $\Omega > S$ often appears

Table 1
Model equations for LK and MMK models (Launder and Kato, 1993; Tsuchiya et al., 1997)

1. Standard $k$–$\varepsilon$ model

$$P_k = \nu_t S^2 \quad (\nu_t : \text{Eq. (5)}) \tag{4}$$

$$\nu_t = C_\mu \frac{k^2}{\varepsilon} \tag{5}$$

$$S = \sqrt{\frac{1}{2}\left(\frac{\partial\langle u_i\rangle}{\partial x_j} + \frac{\partial\langle u_j\rangle}{\partial x_i}\right)^2} \tag{6}$$

2. LK model

$$P_k = \nu_t S\Omega \quad (\nu_t : \text{Eq. (5)}) \tag{7}$$

$$\Omega = \sqrt{\frac{1}{2}\left(\frac{\partial\langle u_i\rangle}{\partial x_j} - \frac{\partial\langle u_j\rangle}{\partial x_i}\right)^2} \tag{8}$$

3. MMK model

$$P_k = \nu_t S^2 \quad (\nu_t : \text{Eqs. (10) or (11)}) \tag{9}$$

$$\nu_t = C_\mu^* \frac{k^2}{\varepsilon}, \quad C_\mu^* = C_\mu \frac{\Omega}{S} \quad \left(\frac{\Omega}{S} < 1\right) \tag{10}$$

$$\nu_t = C_\mu^* \frac{k^2}{\varepsilon}, \quad C_\mu^* = C_\mu \quad \left(\frac{\Omega}{S} \geqslant 1\right) \tag{11}$$

around a bluff body. This drawback of the LK model became more serious in the analysis of flowfield where several bluff bodies were arranged, as the area $\Omega > S$ increased in this situation. The second drawback of the LK model is a mathematical inconsistency in the modeling of Reynolds stress $-\langle u_i' u_j' \rangle$ and $P_k$. In the transport equation of mean flow energy $K\,(=\langle u_i\rangle\langle u_i\rangle/2)$, there is a term which has the same form as that of $P_k$ with the opposite sign. This term plays a role in transferring the kinetic energy from mean flow to turbulence. In the case of the original LK model, the term corresponding to $P_k$ in the equation of mean flow energy $K$ did not take the same form as $P_k$ in the equation of turbulent energy $k$. This is because the LK model only revised the expression of $P_k$ in the equation of $k$. Therefore, $P_k$ in the equation of mean flow energy $K$ and that in the equation of turbulent energy $k$ did not appear in the same form.

Tsuchiya et al. (1997) proposed a new revision of the $k$–$\varepsilon$ model, i.e. MMK model, which corrected these two drawbacks in the LK model, by adding the modification not to the expression for $P_k$ but to the expression for eddy viscosity, $\nu_t$ (cf. Eqs. (10)–(11) in Table 1).

### 2.4.2. *New $k$–$\varepsilon$ models adjusting the turbulence time-scale*

Recently, new types of revised $k$–$\varepsilon$ models, in which the turbulence time-scale is adjusted in accordance with the property of predicted flowfield, have been proposed.

In $k$–$\varepsilon$ models, the eddy viscosity, $\nu_t$, was expressed as

$$\nu_t = C_\mu k \tau \tag{12}$$

where $\tau$ in Eq. (12) was the turbulence time-scale. In the standard $k$–$\varepsilon$ model,

$$\tau = \frac{k}{\varepsilon} \tag{13}$$

Durbin proposed Eq. (14) for $\tau$ based on the "realizability" constraint, $0 \leqslant \langle u_\alpha' u_\alpha' \rangle \leqslant 2k$ via a bound on the time-scale, $\tau$, where summation was not taken in $\langle u_\alpha' u_\alpha' \rangle$ (Durbin, 1996).

The proposed bound on the time-scale is

$$\tau = \min(\tau_u, \tau_D) \tag{14}$$

where

$$\tau_u = \frac{k}{\varepsilon} \tag{15}$$

$$\tau_D = \frac{1}{C_\mu \sqrt{6|S|^2}} \tag{16}$$

$|S|^2 = S_{ij} S_{ij}$ and $S_{ij}$ is the rate of mean strain tensor given by

$$S_{ij} = \frac{1}{2}\left(\frac{\partial \langle u_i \rangle}{\partial x_j} + \frac{\partial \langle u_j \rangle}{\partial x_i}\right). \tag{17}$$

The present authors applied this model to flow past a bluff body and confirmed that its result showed agreement with experimental data better than that obtained using other revised $k$–$\varepsilon$ models (Mochida et al., 2002). However, Lun et al. (2003) pointed out that this model severely over-estimated the size of reverse flow region behind a 2D hill.

Another type of revised model adjusting the turbulence time-scale was proposed by Nagano and Hattori (2003). This model introduced a mixed time-scale ($\tau_\mathrm{m}$), which is a harmonic balance of the turbulent time-scale $\tau_u = k/\varepsilon$ and the time-scale of mean velocity gradient. Various expressions for estimating $\tau_{\mathrm{m}}$, namely $S$ model, $\Omega$ model and $S$–$\Omega$ model were proposed and tested.

$$\frac{1}{\tau_{\mathrm{m}}} = \frac{1}{2}\left(\frac{1}{\tau_u} + \frac{C_S}{\tau_S}\right) \quad (S\text{ model}) \tag{18a}$$

$$\frac{1}{\tau_{\mathrm{m}}} = \frac{1}{2}\left(\frac{1}{\tau_u} + \frac{C_S}{\tau_\Omega}\right) \quad (\Omega\text{ model}) \tag{18b}$$

$$\frac{1}{\tau_{\mathrm{m}}} = \frac{1}{2}\left(\frac{1}{\tau_u} + \frac{C_S}{\tau_{S-\Omega}}\right) \quad (S-\Omega\text{ model}) \tag{18c}$$

where

$$\tau_S = \frac{1}{\sqrt{|S|^2}} \tag{19a}$$

$$\tau_\Omega = \frac{1}{\sqrt{|\Omega|^2}} \tag{19b}$$

$$\tau_{S-\Omega} = \frac{2}{\sqrt{|S|^2} + \sqrt{|\Omega|^2}} \tag{19c}$$

$$|\Omega|^2 = \Omega_{ij}\Omega_{ij} \tag{20}$$

$$\Omega_{ij} = \frac{1}{2}\left(\frac{\partial\langle u_i\rangle}{\partial x_j} - \frac{\partial\langle u_j\rangle}{\partial x_i}\right) \tag{21}$$

and $C_S = 0.4$.

In these models, $\tau$ in Eq. (12) was replaced by $\tau_{\mathrm{m}}$, derived from Eqs. (18a)–(18c). The performances of these models for flow over hilly terrain (Lun et al., 2003; Murakami et al., 2003a) and flow around a cube (Shirasawa et al., 2006) have been examined by the present authors. Fig. 2 shows the vertical profiles of mean streamwise velocity at various positions over a 2D hill model, in comparison with experimental results. A revised $k$–$\varepsilon$ model

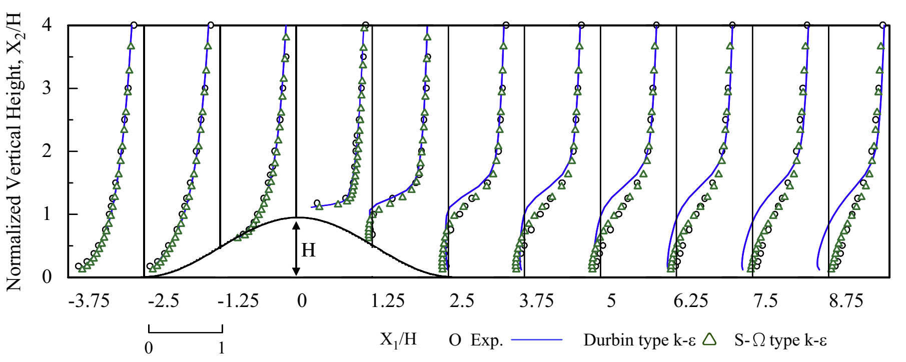


Fig. 2. Comparison of mean streamwise velocity around a 2D hill model (Lun et al., 2003; Murakami et al., 2003a).

Table 2
New model for sensible and latent heat fluxes including buoyancy effects (Yoshida et al., 2000)

1. Sensible heat flux

$$-\langle u_3'\theta'\rangle = \frac{\nu_t}{\sigma_\theta}\frac{\partial\langle\theta\rangle}{\partial x_3} + \frac{k}{\varepsilon}C_{\theta 3}g_3\beta\langle\theta'^2\rangle \quad (22)$$

2. Latent heat flux

$$-\langle u_3'q_w'\rangle = \frac{\nu_t}{\sigma_w}\frac{\partial\langle q_w\rangle}{\partial x_3} + \frac{k}{\varepsilon}C_{\theta 3}g_3\beta\langle\theta' q_w'\rangle \quad (23)$$

$q_w$: mixing ratio of total water
$g_3 = -9.8\,\mathrm{m/s^2}$, $C_{\theta 1} = 0.25$, $C_{\theta 3} = 0.25$, $\sigma_\theta = 0.5$, $\sigma_w = 0.5$

proposed by Durbin (1996) and the $S$–$\Omega$ model proposed by Nagano and Hattori (2003) were employed in this simulation. It was clearly shown that the result of Durbin model deviated from experiment in the region behind the hill. A large re-circulation occurred downstream of the hill. This re-circulation zone was rectified by the newly proposed $S$–$\Omega$ model. $S$–$\Omega$ model was incorporated into the Local Area Wind Energy Prediction System (LAWEPS) developed by Murakami et al. (2003a, c).[1]

#### 2.4.3. Revision of $k$–$\varepsilon$ model incorporating the buoyancy effects on turbulent diffusion

In recent years, the quality of outdoor thermal environment has been regarded as important as that of indoor thermal environment, and a lot of CFD analyses of outdoor thermal environment have been conducted. Since the temperature difference between urban surfaces is large, the effects of buoyancy on turbulent diffusion should be carefully incorporated in this type of analysis, and the conventional $k$–$\varepsilon$ models based on the Eddy-viscosity Concept are clearly inadequate. The present authors have adopted the WET model proposed by Launder (1988) and the revised $k$–$\varepsilon$ model including buoyancy effects, as shown in Table 2, for the analysis of outdoor climate (Yoshida et al., 2000). The revised $k$–$\varepsilon$ model in Table 2 was derived from the simplification of the WET model.

### 2.5. AIJ collaborative research project-cross comparisons of CFD results for wind environment at pedestrian level

Recently, the prediction of wind environment around a high-rise building, using CFD technique, was carried out at the practical design stage. There are a large number of previous studies for the wind environment around actual buildings using CFD (Stathopoulos and Baskaran, 1996; Timofeyef, 1998; Westbury et al., 2002; Richards et al., 2002; Blocken et al., 2003, Yang et al., 2006). However, the influences of the computational conditions; grid discretization, domain sizes and boundary conditions, for instance, on the prediction accuracy of the velocity distribution at pedestrian level near the

[1]The works involved in this project are divided into three phases. During the initial phase of the study, a multi-step wind simulation with nesting method was designed. In the second phase of the work, each submodel was coded and evaluated. Data of observations and experiments were obtained in parallel and used for verification with computation. In the final phase of the project, the performance of the entire simulation system, LAWEPS, was tested and examined by comparing its results with measured data (Murakami et al., 2003a, c).

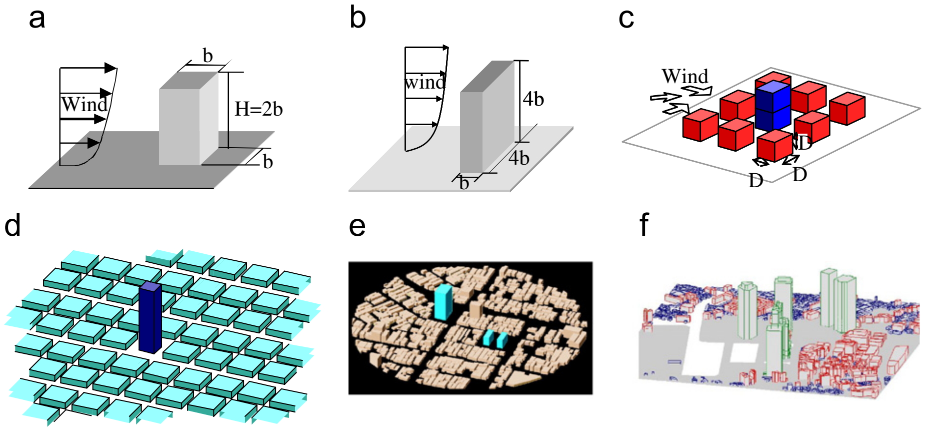


Fig. 3. Six test cases for comparison. (a) Test Case A (2:1:1 square prism). (b) Test Case B (4:4:1 square prism). (c) Test Case C (simple city block). (d) Test Case D (a high-rise building in city). (e) Test Case E (building complexes in actual urban areas (Niigata)). (f) Test Case F (building complexes in actual urban areas (Shinjuku)).

ground have not been systematically investigated. For the aspect of industrial CFD applications, some published policy statements and guidelines have provided valuable information on the application of CFD for pedestrian wind environment around buildings (Roache et al., 1986; AIAA, 1998; ERCOFTAC, 2000) but the guideline oriented to the application of this area is somehow different. Recently, the recommendations on the use of CFD in predicting pedestrian wind environment were proposed by the COST C14 group (Franke et al., 2004, Franke, 2006), these recommendations were mainly based on the results published elsewhere.

In view of this point, a working group for CFD prediction of wind environment around buildings, which consisted of researchers from several universities and private companies,[2] was organized by the Architectural Institute of Japan (AIJ). During initial stage of that project, the working group carried out cross comparisons of CFD results for flow around a single high-rise building, building block placed within the surface boundary layer and flow within a building complex in urban area, obtained from various $k$–$\varepsilon$ models, DSM and LES (Mochida et al., 2002; Tominaga et al., 2004; Yoshie et al., 2005a, b; Tominaga et al., 2005, 2006; Yoshie et al., 2006). Fig. 3 illustrates the six (a–f) test cases for these cross comparisons. They were carried out to clarify the major factors which affect the prediction accuracy. In order to assess the performance of turbulence models, the results should be compared under the same computational conditions. Special attention was given to this point, in this project. The computational conditions, i.e. grid arrangements, boundary conditions, etc., were specified by the organizers and participants in this project were

[2]The CFD Working Group members are: A. Mochida (Chairman, Tohoku University), Y. Tominaga (Secretary, Niigata Institute of Technology), Y. Ishida (I.I.S., University of Tokyo), T. Ishihara (University of Tokyo), K. Uehara (National Institute of Environmental Studies), R. Ooka (I.I.S., University of Tokyo), H. Kataoka (Obayashi Corporation), T. Kurabuchi (Tokyo University of Science), N. Kobayashi (Tokyo Institute of Polytechnics), T. Shirasawa (Tokyo Polytechnic University), N. Tuchiya (Takenaka Corporation), Y. Nonomura (Fujita Corporation), T. Nozu (Shimizu Corporation), K. Harimoto (Taisei Corporation), K. Hibi (Shimizu Corporation), S. Murakami (Keio University), T. Yamanaka (Kajima Corporation), R. Yoshie (Tokyo Polytechnic University), M. Yoshikawa (Taisei Corporation).

Table 3
Computed cases for 2:1:1 shaped building model (Test Case A)

| Affiliation | Case | Software | Turbulence model | Scheme for convection terms | Computational method and time integral scheme | $X_R$[a]/$b$ | $X_F$[b]/$b$ |
|---|---|---|---|---|---|---|---|
| A | KE1 | STREAM ver.2.10 | $k$–ε (standard) | QUICK | SIMPLE, steady solution | – | 2.54 |
| B | KE2 | STREAM ver.2.10 | $k$–ε (standard) | QUICK (First-order upwind for $k$ and ε) | SIMPLE, steady solution | – | 1.66 |
| C | KE3 | STREAM ver.2.10 | $k$–ε (standard) | QUICK | SIMPLE, steady solution | – | 2.00 |
| | LK1 | | $k$–ε (LK) Launder and Kato (1993) | | | 0.87 | 2.98 |
| D | KE4 | STREAM ver.2.10 | $k$–ε (standard) | QUICK | SIMPLE, steady solution | – | 2.00 |
| | RNG1 | | $k$–ε (RNG) Yakhot and Orsag (1986) | QUICK | | 0.50 | 2.80 |
| E | KE5 | STAR-LT ver.2.0 | $k$–ε (standard) | QUICK | SIMPLE, steady solution | – | 2.20 |
| F | MMK1 | Homemade | $k$–ε (MMK) Tsuchiya et al. (1997) | QUICK | MAC, unsteady solution with implicit scheme | 0.65 | 2.72 |
| G | KE6 | FLUENT ver.5.0 | $k$–ε (standard) | Central | SIMPLE, steady solution | – | 2.41 |
| | RNG2 | | $k$–ε (RNG) Yakhot and Orsag (1986) | | | 0.58 | 3.34 |
| | KE8 | Homemade | $k$–ε (standard) | QUICK | HSMAC, unsteady solution with implicit scheme | – | 2.70 |
| | LK2 | | $k$–ε (LK) Launder and Kato (1993) | | | 0.58 | 3.19 |
| | LK3 | | $k$–ε (modified LK) Tominaga and Mochida (1999) | | | 0.53 | 3.11 |
| | MMK2 | | $k$–ε (MMK) Tsuchiya et al. (1997) | | | 0.52 | 3.09 |
| | DBN | | $k$–ε (Durbin, 1996) | | | 0.63 | 2.70 |
| | DSM | | DSM Murakami et al. (1993) | | | >1.0 | 4.22 |
| | LES1 | | LES (without inflow turbulence) Tominaga et al. (2003) | Second-order centered difference | SMAC, Convection terms: Adams-Bashforth scheme | 0.62 | 1.02 |
| | LES2 | | LES (with inflow turbulence) Tominaga et al. (2003) | | Diffusion terms: Crank-Nicolson scheme | 0.50 | 2.10 |
| H | KE7 | Homemade | $k$–ε (standard) | QUICK | HSMAC, unsteady | – | 1.98 |

Table 3 (*continued*)

| Affiliation | Case | Software | Turbulence model | Scheme for convection terms | Computational method and time integral scheme | $X_R{}^a/b$ | $X_F{}^b/b$ |
|---|---|---|---|---|---|---|---|
| | | | | | solution with implicit scheme | | |
| I | DNS | Homemade | DNS Kataoka and Mizuno (2002) | Third-order upwind scheme | Artificial compressibility method, explicit | 0.92 | 2.05 |
| | Experiment | | | | | 0.52 | 1.42 |

[a] $X_R$: Reattachment length on the roof.
[b] $X_F$: Reattachment length behind the building.

requested to follow these conditions. Two representative cases, Cases A and E, are discussed next.

*2.5.1. Test Case A (2:1:1 shaped building model)*

A summary of computations carried out for 2:1:1 shaped building model (Test Case A) is provided in Table 3. Nine groups have submitted a total of 18 data sets of computational results. The performance of the standard $k$–$\varepsilon$ and five types of revised $k$–$\varepsilon$ models was examined. Furthermore, Differential Stress Model (DSM) (Murakami et al., 1993), Direct Numerical Simulation (DNS) with third-order upwind scheme (Kataoka and Mizuno, 2002) and large eddy simulation (LES) using the Smagorinsky SGS model (Tominaga et al., 2003) were also included in the comparison.

The predicted reattachment lengths on the roof, $X_R$, and that behind the building, $X_F$, were determined for all the cases, as shown in Table 3. It can be seen that the reverse flow on the roof, clearly observed in the experiment, was not reproduced using the standard $k$–$\varepsilon$ (KE1–8). On the other hand, the reverse flow on the roof appeared in the results of all the revised $k$–$\varepsilon$ models (LK1, RNG1, MMK1, RNG1, LK2, LK3, MMK2, DBN), though its size was slightly larger than that of the experiment. In the DSM result, the separated flow from a windward corner was predicted too large, and it did not reattach on the roof. The result of LES without inflow turbulence (LES1) can reproduce the reattachment on the roof, but $X_R$ is somewhat over-estimated in this case. On the other hand, the result of LES with inflow turbulence (LES2) shows close agreement with the experiment.

The reattachment length behind the building, $X_F$, computed using the standard and revised $k$–$\varepsilon$ models was larger than the experimental value, in all the cases. It is surprising to see that there were significant differences in $X_F$ values between the results obtained using the standard $k$–$\varepsilon$ model. As was already noted, the grid arrangements and boundary conditions were set to be identical in all cases, and QUICK scheme was used for convection terms, in many cases. The reason for the difference in $X_F$ values predicted by the standard $k$–$\varepsilon$ models is not clear, but it may be partly due to the difference in some details of numerical conditions, e.g. the convergence criteria, etc. The results of the revised $k$–$\varepsilon$ models, except for the Durbin model, led to $X_F$ larger than the value obtained using the standard $k$–$\varepsilon$ model. The computational–experimental discrepancy was significantly lower for LES and DNS computations. On the other hand, DSM greatly over-estimated $X_F$. The over-estimation of the reattachment length behind a 3D obstacle was also reported by Lakehal and Rodi (1997).

The size of the recirculation region behind the building is strongly affected by the momentum transfer mechanism in the wake region, where vortex shedding plays an important role. Thus, the reproduction of vortex shedding is important for accurate prediction of $X_F$ value. However, none of the $k$–$\varepsilon$ models compared here could reproduce vortex shedding. This resulted in underestimation of the mixing effects in the lateral direction causing a large re-circulation region behind the building.

### *2.5.2. Test Case E (building complex in actual urban area)*

Prediction accuracy for wind environment within an actual building complex, located in Niigata City, Niigata Prefecture, Japan, was examined in this test case. The prediction was carried out by three different codes, namely an in-house developed CFD code and two commercial CFD codes. The computational conditions are given in Table 4. In order to reproduce the geometries of the surrounding building blocks, data from an identical CAD file was used in the three codes. This file was produced from the drawings of the experimental model.

Although CFD simulations have been performed for 16 different wind directions, only the wind distributions for wind directions of NNE and W, which are the prevailing wind directions in Niigata City, are shown here. Since there were no clear differences between the horizontal distributions of wind speed near ground surface, predicted

Table 4
Computed cases for building complex in actual urban area (Test Case E)

| CFD code | Code O, self-made code | Code M, commercial code | Code T, commercial code |
|---|---|---|---|
| Computational method and time integral scheme | Overlapping structured grid | Structured grid | Unstructured grid |
| | Artificial compressibility | SIMPLE, steady state | SIMPLE, steady state |
| Turbulence model | Standard $k$–$\varepsilon$ | Standard $k$–$\varepsilon$ | Standard $k$–$\varepsilon$ |
| Scheme for advection term | Third-order upwind | QUICK | MUSCL (Second-order) |
| Grid arrangements | 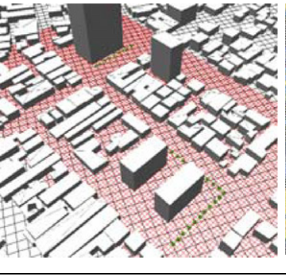 | 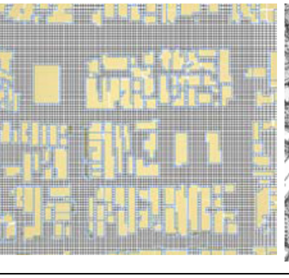 | 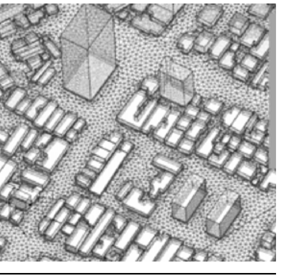 |

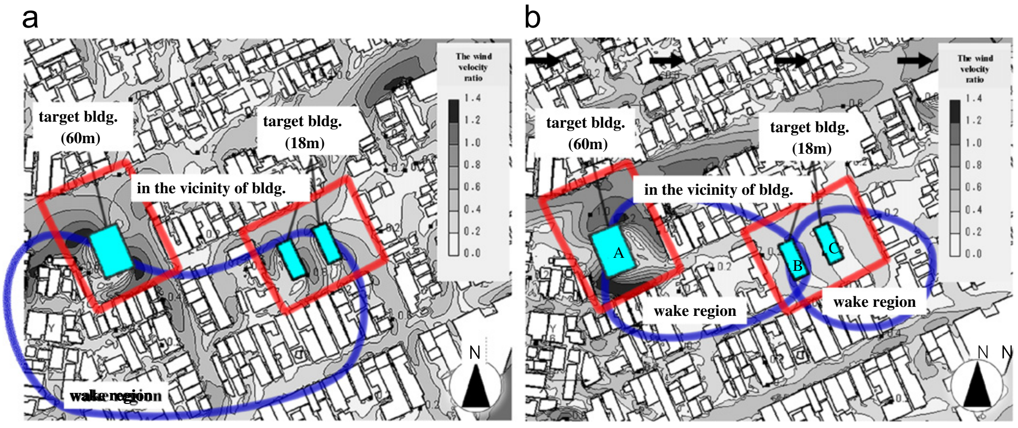


Fig. 4. Distributions of scalar velocity near ground surface around building complex (Tominaga et al., 2004, 2005, 2006; Yoshie et al., 2005a, b, 2006). (a) Wind direction: NNE; (b) Wind direction: W.

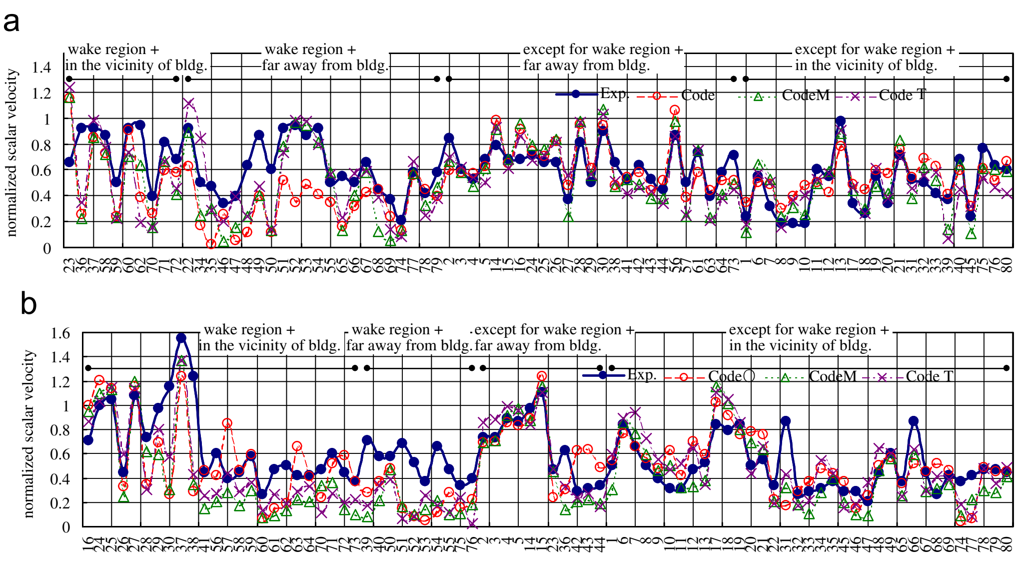


Fig. 5. Comparison of scalar velocity value for each measurement (Tominaga et al., 2004, 2005, 2006; Yoshie et al., 2005a, b, 2006). (a) Wind direction: NNE; (b) Wind direction: W.

by the three CFD codes, only the results obtained using Code T are presented (cf. Fig. 4). This figure illustrates the horizontal distributions of scalar velocity near ground surface ($z = 2\,\mathrm{m}$). The values in Fig. 4 are normalized by the velocity value at the same height at inflow boundary. Fig. 5 shows a comparison of CFD results with wind tunnel experiments. It was found that the scalar velocity predicted by all CFD codes was smaller in the wake region compared to the experimental value. This discrepancy is mainly due to the fact that $k$–$\varepsilon$ model cannot reproduce the vortex shedding from tall buildings, similarly as in Test Case A. This problem is absent in LES results, but the computational cost of adopting LES is still beyond the scope of practical applications. In order to overcome this drawback, the adaptation of hybrid RANS/LES and DES (detached-eddy simulation) (Spalart, 1999; Menter and Kunts, 2001; Squires, 2003; Kenjers and Hanjalic, 2005) would be needed. The current state of these approaches was shown in the invited lectures presented during CWE2006 by Hanjalic and Kenjers(2006) and Squires (2006).

## 3. Modeling of small scale flow obstacles

### 3.1. Various SGS obstacles in real situations

The real situations of environment in street canyons are influenced by the interaction of various objects, both stationary and non-stationary. In most of the previous CFD simulations of flow around buildings, only the influences of topographic features and building geometry were considered (cf. Fig. 1(1)). At the pedestrian level, influences of small obstacles such as trees (stationary) and automobiles (non-stationary) are significant (cf. Figs. 1(2) and (3)). Their effects have been neglected in most of conventional CFD predictions of wind environment. However, modeling of the effects of such SGS flow obstacles have been investigated in recent years by many researchers.

### 3.2. Modeling of aerodynamic and thermal effects of tree canopy

#### 3.2.1. Outline of tree canopy model for reproducing various effects of planted trees

Tree planting is one of the most popular measures of environmental design for improving outdoor climate. It reduces strong wind around high-rise buildings, improves outdoor thermal comfort, etc. In order to reproduce the effects of trees, a lot of researches have been conducted (Yamada, 1982; Uno et al., 1989; Svensson and Häggkvist, 1990; Green, 1992; Hiraoka, 1993; Liu et al., 1996; Hiraoka, 2004; Mochida et al., 2006b; Ohashi, 2004; Hiraoka and Ohashi, 2006; Yoshida et al., 2006). Prof. Hiraoka is one of the pioneers in this research field. He has developed models for expressing aerodynamic effects of trees, stomatal conductance, radiative heat transfer, balance of heat, water vapor and carbon dioxide within vegetation canopy (Hiraoka, 2004). The present model developed by Hiraoka is very comprehensive and can provide very accurate prediction of microclimate within vegetation canopy, provided that proper input parameters are given. From the viewpoint of engineering application, however, it is usually not easy to apply this model because it requires too many input parameters, some of which are usually not available now. Yoshida et al. (2006) developed a 3D tree canopy model which can be easily applied to the practical applications related to microscale climate prediction. It includes the following effects (cf. Fig. 6):

(1) aerodynamic effects of planted trees;
(2) thermal effects;
   - shading effects on short-wave and long-wave radiations;
   - productions of water vapor (latent heat) and sensible heat from planted trees.

Yoshida et al. predicted the effects of tree planting on outdoor thermal comfort by using coupled simulation of convection (CFD) and radiation combined with the tree

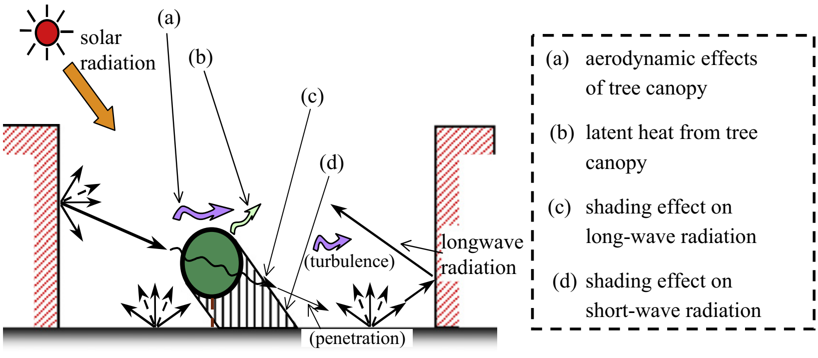


Fig. 6. Effects of tree considered in the tree canopy model (Yoshida et al., 2006).

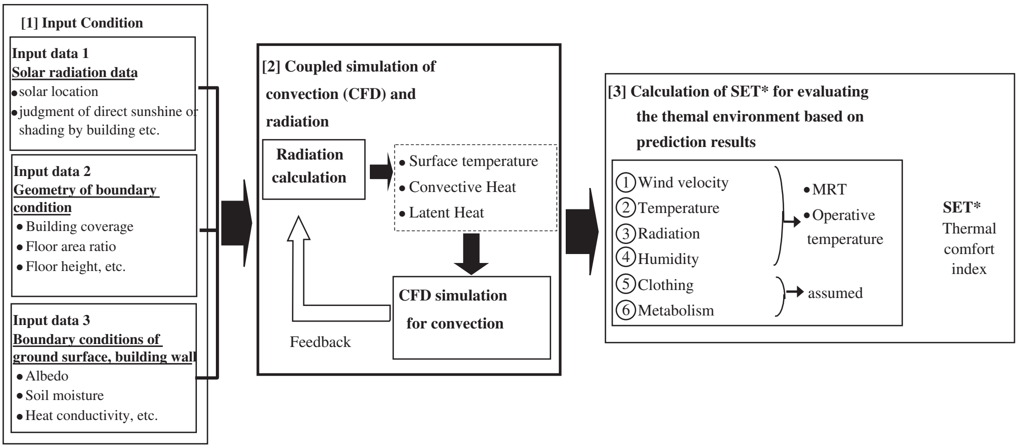


Fig. 7. Flowchart for assessing outdoor human comfort based on CFD (Yoshida et al., 2000, 2006).

Table 5
Additional terms for tree canopy (Yoshida et al., 2006)

$$F_i = -\eta C_f a(x_1, x_2, x_3)\overline{\langle u_i \rangle}\sqrt{\overline{\langle u_j \rangle}^2} \tag{24}$$

$$F_k = \overline{\langle u_i \rangle} F_i \tag{25}$$

$$F_\varepsilon = \frac{\varepsilon}{k} C_{p\varepsilon} F_i \tag{26}$$

$\eta$: green coverage ratio, $C_f$: drag coefficient, $a(x_1,x_2,x_3)$: leaf surface area density, $\langle f \rangle$: ensemble-average, $\bar{f}$: spatial-average or filtered quantities.

canopy model (Yoshida et al., 2006). Fig. 7 illustrates the outline of computational approach for predicting outdoor thermal comfort. Four equations: (1) transport equation of momentum, (2) transport equation of heat, (3) transport equation of moisture,

Table 6
Heat balance equations of plant canopy (Yoshida et al., 2006)

$$S_P + R_{DP} + H_P + LE_P = 0 \tag{27}$$

$$H_P = A_P \alpha_C (T_{aP} - T_P) \tag{28}$$

$$LE_P = A_P \alpha_W \beta_P L (f_{aP} - f_{sP}) \tag{29}$$

where $S_P$: absorbed solar radiation flux on leaf surfaces (W), $R_{DP}$: absorbed longwave radiation flux on leaf surfaces (W), $H_P$: sensible heat on leaf surfaces (W), $LE_P$: latent heat on leaf surfaces (W), $L$: latent heat of water vaporization ($2.5 \times 10^6$ J/kg), $A_P$: leaf area within tree crown ($A_P$ is twice the product of the volume of tree crown and the leaf area density of tree crown) ($m^2$), $\alpha_C$: convective heat transfer coefficient on leaf surfaces ($W/m^2 K$), $T_P$: leaf surface temperature (K), $T_{aP}$: air temperature in the mesh including tree crown (K), $\alpha_W$: convective moisture transfer coefficient on leaf surfaces ($kg/(m^2 s\,kPa)$), ($\alpha_W = 7.0 \times 10^{-6} \alpha_C$), $\beta_P$: moisture availability on leaf surfaces, (−), $f_{aP}$: water vapor pressure in the mesh including tree crown (kPa), $f_{sP}$: saturation water vapor pressure at leaf surface temperature (kPa).

and (4) heat transfer equation by radiation are solved as a system of coupled equations.

This 3D canopy model employed the $k$–$\varepsilon$ turbulence model, with extra terms (cf. Table 5) added into the transport equations, to simulate the aerodynamic effects of trees. The term "$-F_i$" included in the $i$ component of momentum equation denotes the drag force. "$+F_k$" and "$+F_\varepsilon$" are added, respectively, into the transport equations for turbulent kinetic energy, $k$, and energy dissipation rate, $\varepsilon$, to represent the effects of trees on turbulent flowfield. These extra terms were derived by applying the spatial average to the basic equation (Hiraoka, 1993). The radiative heat transport was computed using the method based on Monte-Carlo simulation (Omori et al., 1990). The solar and longwave radiant fluxes incident to the plant canopy were calculated by assuming a decay rate of $\{1-\exp(-k' a(x_1,x_2,x_3) l)\}$, where $k'$ is the absorption coefficient and $l$ is the length by which radiant flux passes through the plant canopy. The mean leaf surface temperature of the plant canopy was estimated using the heat balance equations listed in Table 6. In the heat balance equation (27), the heat conductivity term is neglected, as heat capacity of leaf was negligibly small.

Results obtained using this model were presented by Yoshida et al. (2006). Based on similar approaches, various studies have been conducted in recent years to investigate the effects of planted trees on outdoor thermal environment and optimize their shapes, densities and layouts (Mochida et al., 2005; Ooka et al., 2006; Lin et al., 2006).

### 3.2.2. *Optimization of tree canopy model for reproducing the aerodynamic effects*

Recently, the present authors carried out a series of numerical studies to examine the accuracy of the existing canopy models in reproducing the aerodynamic effects of trees, and to optimize the model coefficients (Murakami et al., 2003a; Mochida et al., 2006b). The canopy models adopted in these studies used the revised $k$–$\varepsilon$ model, which based on a "mixed time-scale" concept ($S$–$\Omega$ model), as a base, with extra terms added into the transport equations as shown in Table 5. The additional terms contained four parameters, $C_{p\varepsilon}$, $\eta$, $a$ and $C_f$. "$C_{p\varepsilon}$" was regarded as a model coefficient in turbulence modeling for prescribing the time-scale of the process of energy dissipation in the canopy layer, while

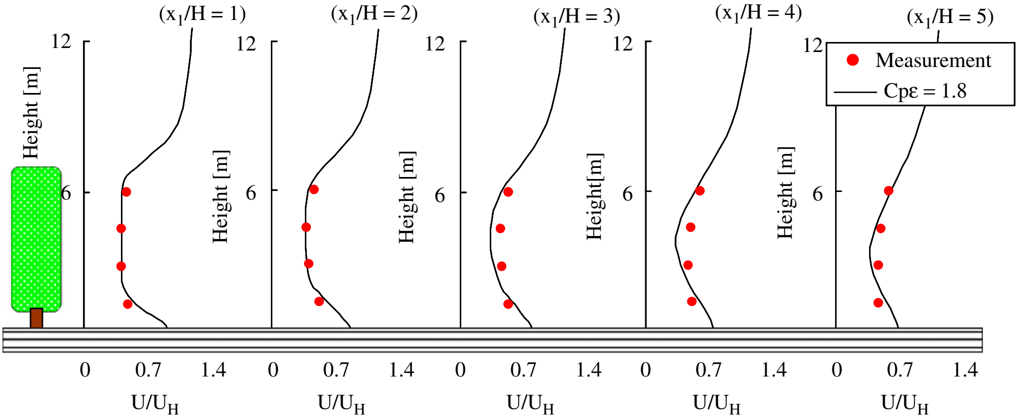


Fig. 8. Comparison of normalized vertical profiles of mean streamwise velocity behind pine trees ($H$: a height of tree, $U_H$: inflow velocity at a height of $H$) (Mochida et al., 2006b).

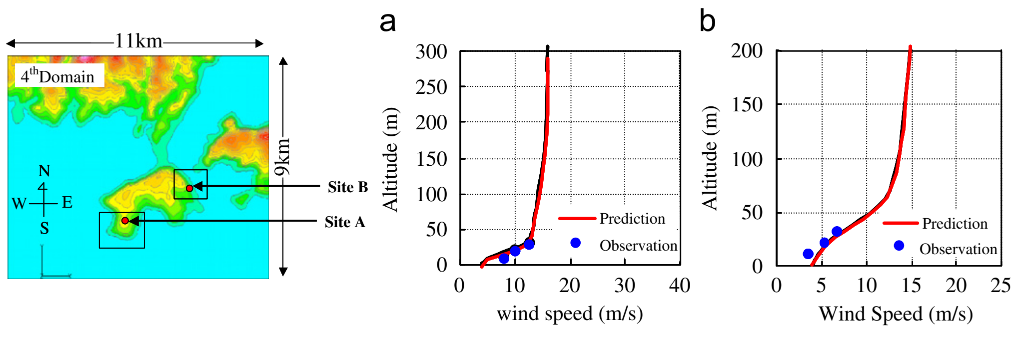


Fig. 9. Comparison of vertical velocity profiles above Shionomisaki Peninsular, Wakayama, Japan (December 15th, 15JST, 2001) (Murakami et al., 2003b). (a) Site A and (b) Site B.

"$\eta$", "$a$" and "$C_f$" were the parameters which should be determined according to the conditions of trees. The choice of value of $C_{p\varepsilon}$ in $F_\varepsilon$ (cf. Eq. (26) in Table 5) strongly affects the prediction accuracy (Mochida et al., 2006b), and considerable differences were observed between the values adopted in the previous researches (Yamada, 1982; Uno et al., 1989; Svensson and Häggkvist, 1990; Green, 1992; Hiraoka, 1993; Liu et al., 1996; Hiraoka, 2004; Mochida et al., 2006b; Ohashi, 2004; Yoshida et al., 2006). The $C_{p\varepsilon}$ was optimized by the present authors and the predicted results were compared with experimental results as shown in, for an example, Fig. 8. The value of 1.8 was selected for $C_{p\varepsilon}$ as a result of a series of numerical experiments. The tree canopy model developed here was incorporated in the LAWEPS (Murakami et al., 2003a, c). A five-stage nesting grid system was adopted in the LAWEPS. The largest domain (1st Domain) covered an approximate region on a scale about 500 km × 500 km in horizontal plane, and 10 km in vertical direction. The smallest domain (5th domain) occupied region of about 1 km × 1 km × 1 km.Figs. 9(1) and (2) compare the vertical velocity profiles predicted by LAWEPS with the tower observations at Shionomisaki Peninsular, Wakayama, Japan

Table 7
Additional terms in various tree canopy models

| $F_i$ | | $F_k$ | $F_\varepsilon$ | Selected values for numerical coefficients |
|---|---|---|---|---|
| Type A | $\eta C_f \overline{a\langle u_i\rangle}\sqrt{\overline{\langle u_j\rangle}^2}$ | $\overline{\langle u_i\rangle}F_i$ | $\eta\frac{\varepsilon}{k}\cdot C_{p\varepsilon1}\frac{k^{3/2}}{L}\ \ (L=\frac{1}{a})$ | Hiraoka (1993): $C_{p\varepsilon1}=0.8{\sim}1.2$ |
| Type B | $\eta C_f \overline{a\langle u_i\rangle}\sqrt{\overline{\langle u_j\rangle}^2}$ | $\overline{\langle u_i\rangle}F_i$ | $\frac{\varepsilon}{k}\cdot C_{p\varepsilon1}F_k$ | Yamada (1982): $C_{p\varepsilon1}=1.0$ |
| | | | | Uno et al. (1989): $C_{p\varepsilon1}=1.5$<br>Svensson and Häggkvist, 1990: $C_{p\varepsilon1}=1.95$ |
| Type C | $\eta C_f \overline{a\langle u_i\rangle}\sqrt{\overline{\langle u_j\rangle}^2}$ | $\overline{\langle u_i\rangle}F_i-4\eta C_f a\sqrt{\overline{\langle u_j\rangle}^2}$ | $\frac{\varepsilon}{k}\left[C_{p\varepsilon1}\left(\overline{\langle u_i\rangle}F_i\right)-C_{p\varepsilon2}\left(4\eta C_f a\sqrt{\overline{\langle u_j\rangle}^2}\right)\right]$ | Green (1992): $C_{p\varepsilon1}=C_{p\varepsilon2}=1.5$ |
| | | | | Liu et al. (1996): $C_{p\varepsilon1}=1.5$, $C_{p\varepsilon2}=0.6$ |
| Type D | $\eta C_f \overline{a\langle u_i\rangle}\sqrt{\overline{\langle u_j\rangle}^2}$ | $\overline{\langle u_i\rangle}F_i-4\eta C_f a\sqrt{\overline{\langle u_j\rangle}^2}$ | $\eta\frac{\varepsilon}{k}\cdot C_{p\varepsilon1}\frac{k^{3/2}}{L}\ \ (L=\frac{1}{a})$ | Ohashi (2004): $C_{p\varepsilon1}=2.5$ |

(Murakami et al., 2003c). It can be seen that the results of numerical prediction show very close agreement with the observations.

The present authors have recently carried out an extensive review on tree canopy models. Four types of canopy models were selected. The model coefficients adopted in the extra term added to the transport equation of energy dissipation rate, $\varepsilon$, were optimized by comparing the numerical results with field measurements. The four selected tree canopy models (Uno et al., 1989; Svensson and Häggkvist, 1990; Green, 1992; Hiraoka, 1993; Liu et al., 1996; Ohashi, 2004) are based on $k$–$\varepsilon$ model as given in Table 7.

As seen in Table 7, the additional terms contain five parameters, two model coefficients, $C_{p\varepsilon1}$ and $C_{p\varepsilon2}$, $\eta$, $a$ and $C_f$. Results with Types B and C models are compared with measurements in a recent paper by Mochida et al. (2006b).

### 3.3. Modeling for aerodynamic effects of vehicle canopy

Recently, the present authors developed a simulation method named "vehicle canopy model" to predict the effects of moving automobiles on flow and diffusion fields within street canyons (Mochida et al., 2006a; Hataya et al., 2006).

#### 3.3.1. Outline of vehicle canopy model

In this model, the effects of each individual moving automobile were not directly modeled. Instead, the total effects of all the moving automobiles in the street were considered as a whole. The aerodynamic effect of the moving automobiles was modeled using the methodology of canopy model. The proposed vehicle canopy model was based on the $k$–$\varepsilon$ model, in which terms were added in the transport equations. Similarly to the tree canopy model (Yamada, 1982; Uno et al., 1989; Svensson and Häggkvist, 1990; Green, 1992; Hiraoka, 1993; Liu et al., 1996; Hiraoka, 2004; Mochida et al., 2006b; Ohashi, 2004; Yoshida et al., 2006), the extra term "$-F_i$" was included in the momentum equation, cf. Table 8, to account for the effect of moving automobiles on velocity change. This "$-F_i$" was defined as a function of wind velocity $\langle u_i\rangle$ in the tree canopy model (cf. Tables 5 and 7). In modeling vehicle canopy, $\langle u_i\rangle$ was replaced by the relative velocity

Table 8
Additional terms for vehicle canopy model (Mochida et al., 2006a; Hataya et al., 2006)

| | |
|---|---|
| $F_i = \frac{1}{2} C_{f\text{-car}} \frac{A_{\text{car}}}{V_{\text{cell}}} (\overline{\langle u_i \rangle} - \overline{\langle u_{i\text{-car}} \rangle}) \sqrt{(\langle u_j \rangle - \overline{\langle u_{j\text{-car}} \rangle})^2}$ | (30) |
| $F_k = (\overline{\langle u_i \rangle} - \overline{\langle u_{i\text{-car}} \rangle}) F_i$ | (31) |
| $F_\varepsilon = \frac{\varepsilon}{k} \frac{k^{3/2}}{L} C_{\varepsilon-\text{car}}$ | (32) |

$C_{f\text{-car}}$: drag coefficient of automobiles, $A_{\text{car}}/V_{\text{cell}}$: ratio of sectional area of automobiles observed from $i$ direction to the fluid volume within the vehicle canopy layer (1/m)

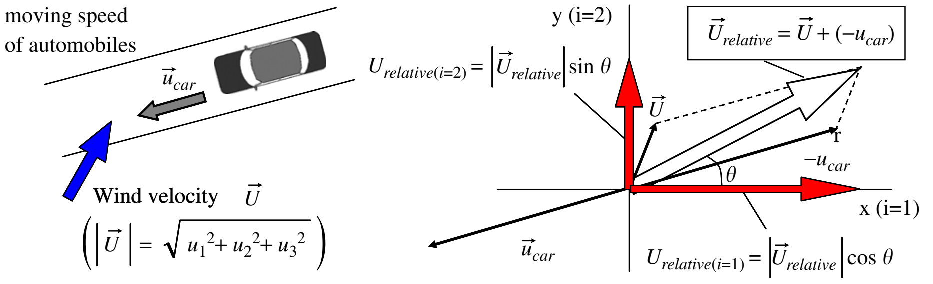


Fig. 10. Relationship between wind velocity and moving speed of automobiles.

Fig. 11. Actual urban space; Jozenji street, Sendai, Japan.

between wind velocity and moving speed of automobiles (cf. Fig. 10). In order to simulate the effects of moving automobiles on turbulence increase rate and energy dissipation rate, additional terms “$+F_k$” and “$+F_\varepsilon$” were included in the transport equations of turbulent kinetic energy, $k$, and energy dissipation rate, $\varepsilon$. Table 8 quantifies these extra terms (Mochida et al., 2006a; Hataya et al., 2006).

Table 9
Test cases for vehicle canopy model (Mochida et al., 2006a; Hataya et al., 2006)

| | Roadside trees | Effects of moving automobiles on turbulent diffusion process |
|---|---|---|
| Case 1 | Without | Without automobiles |
| Case 2 | Present situation | Without automobiles |
| Case 3-1 | Present situation | $u_{car} = 0\,km/h$ |
| Case 3-2 | Present situation | $u_{car} = 15\,km/h$ |

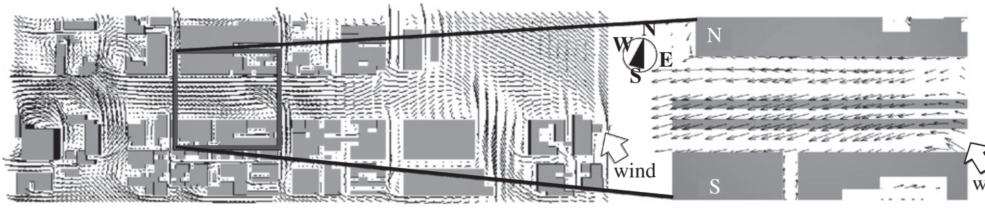


Fig. 12. Horizontal distributions of wind velocity vectors (without trees and automobiles, 12:00 a.m. on August 3rd at a height of 1.5 m) (Mochida et al., 2006a; Hataya et al., 2006).

Table 10
Comparison of turbulent kinetic energy, $k$ ($m^2/s^2$) (Mochida et al., 2006a; Hataya et al., 2006)

| Measuring points | Result of field measurement | Results of CFD analyses | | | |
|---|---|---|---|---|---|
| | | Case 1 | Case 2 | Case 3-1 | Case 3-2 |
| Northern sidewalk | 0.44 | 0.06 | 0.07 | 0.02 | 0.22 |
| Southern sidewalk | 0.27 | 0.12 | 0.03 | 0.03 | 0.25 |

### 3.3.2. CFD analyses of flowfield in real situations in street canyon

By using the proposed vehicle canopy model, the flow and diffusion fields within Jozenji-street in Sendai, Japan, Fig. 11, were predicted. The accuracy of CFD analyses was confirmed by comparing the simulation results with the field measurement results conducted by the present authors (Mochida et al., 2005; Watanabe et al., 2005). Details of the numerical settings can be obtained from Mochida et al. (2006a) and Hataya et al. (2006).

All the test cases are shown in Table 9. Horizontal distributions of wind velocity vectors at a height of 1.5 m for Case 1 are illustrated in Fig. 12. A comparison of the results of turbulent kinetic energy, $k$, between field measurements and CFD analyses in Jozenji-street is given in Table 10. In the cases without automobiles (Cases 1 and 2), $k$ values were largely under-predicted in comparison with the measurement results. However, the magnitude of $k$ due to turbulent diffusion generated by moving automobiles was well reproduced in Case 3-2, especially on the southern sidewalk.

## 3.4. Modeling for aerodynamic and thermal effects of building canopy

Temperature increase due to urbanization is becoming very serious problem in Japan. City administrators and urban planners are now willing to adopt countermeasures that can mitigate the problem of UHI effects. Various urban planning scenarios have been proposed to minimize the impact of urbanization on urban climate. Since the mid-1990s, a lot of numerical studies of mesoscale climate in urban areas have been carried out by many researchers (Mochida et al., 1997; Murakami et al., 2003b; Ooka et al. 2004; Kondo et al., 2006; Sato et al., 2006; Sasaki et al., 2006).

Historically, 1D heat balance model was usually adopted for the ground boundary conditions in mesoscale climate analysis. In this conventional model, a roughness parameter was employed to represent the effect of the building complex. As the vertical grid size adjacent to the ground surface must be made several times larger than the roughness length in the conventional model, physical phenomena within the surface layer could not be estimated. Furthermore, the definition of surface temperature is vague in the conventional model because its relationship with ground, roof and wall surface temperature is unclear. Therefore, it is necessary to include the effects of urban canopy precisely in order to analyze the thermal environment at pedestrian level, in an urban area. On the other hand, the 1D urban canopy model was also commonly used to analyze urban thermal environments. Although this model can predict the thermal environment at pedestrian level easily, it does not make possible to consider the effects of local climate, due to the limitation of the assumption of a horizontally homogeneous flow and temperature field.

Recently, Ooka et al. (2004) developed a comprehensive urban canopy model that considers the following five factors in dealing with building complex: (1) wind reduction by the building complex, (2) production of turbulence by the building complex, (3) solar radiation (short-wave) heat transfer inside and outside the building complex, (4) long-wave radiation heat transfer inside and outside the building complex and (5) sensible and latent heat transfer from the building surfaces. The urban canopy model developed in their study was incorporated into the meteorological mesoscale model. The effects of plant canopy, as illustrated in Fig. 6, were also considered. Concerning the modeling of aerodynamic effects of the building canopy, i.e. (1) and (2), Maruyama (1993) developed a building canopy model, which has been widely used by many researchers. He also provided detailed database obtained by a series of wind tunnel tests to determine the model coefficients included in his model.

## 4. Integration of CWE simulations with various scales

CWE applications now cover various phenomena, at scales ranging from microclimate around a human body to regional climate (cf. Fig. 13). Although scales associated with these phenomena are different, they are related and coupled to each other. Research efforts, thus, should be devoted to develop a method for integrating the submodels into a comprehensive, total simulation system. For this purpose, it is necessary to develop a new software platform which not only can handle many subsystems for analyzing each scale-dependent phenomena, but also can integrate them for evaluating the total urban climate. Fig. 14 illustrates the concept of the platform proposed by Murakami, Mochida and Ooka et al. (Murakami et al., 2000; Murakami, 2004; Mochida, 2005).

A number of case studies based on the proposed software platform were presented by Murakami and the present authors (Murakami, 2004; Mochida, 2005). It was pointed out that CWE is now in the process of growing from a tool for analysis to the tool for environmental design.

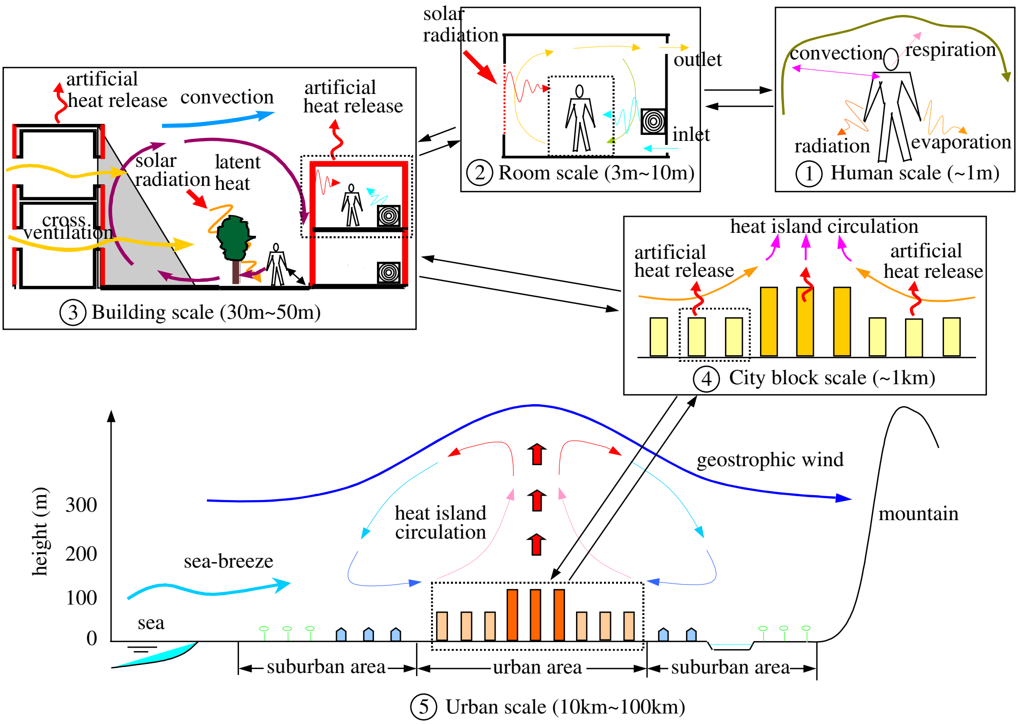


Fig. 13. Various scale phenomena related to wind climate (Murakami et al. 2000; Murakami, 2004).

## 5. Concluding remarks

This paper reviewed the progress in CWE research over the past 10 years, primarily achieved by the researchers in the field of environmental engineering in Japan. The first part of the paper outlined the progress in turbulence modeling for predicting turbulent flow around buildings and wind environment in building complex. In the 1990s, many investigations were carried out to examine the performance of the dynamic LES models based on the dynamic Smagorinsky type, DM type, Lagrangian dynamic type, etc. Various methods for generating inflow turbulence for LES were developed during this time period. Presently, researches to improve the prediction accuracy of $k$–$\varepsilon$ models are still continued. The performance of various revised $k$–$\varepsilon$ models was examined for flow around a bluff body, city building blocks, actual building complex and flow over hilly terrains. It was confirmed that the revised $k$–$\varepsilon$ models which were proposed to correct the drawback of the standard $k$–$\varepsilon$ model that severely over-predicts the turbulence energy, $k$, around front corners could undoubtedly improve the prediction accuracy for computing the strong wind in separated flow regions around front corners. However, all revised $k$–$\varepsilon$ models over-predicted the sizes of reattachment lengths behind buildings and under-predicted the velocity values in the wake regions. This discrepancy is mainly due to the fact that all $k$–$\varepsilon$ models could not reproduce the vortex shedding from buildings. This problem does not

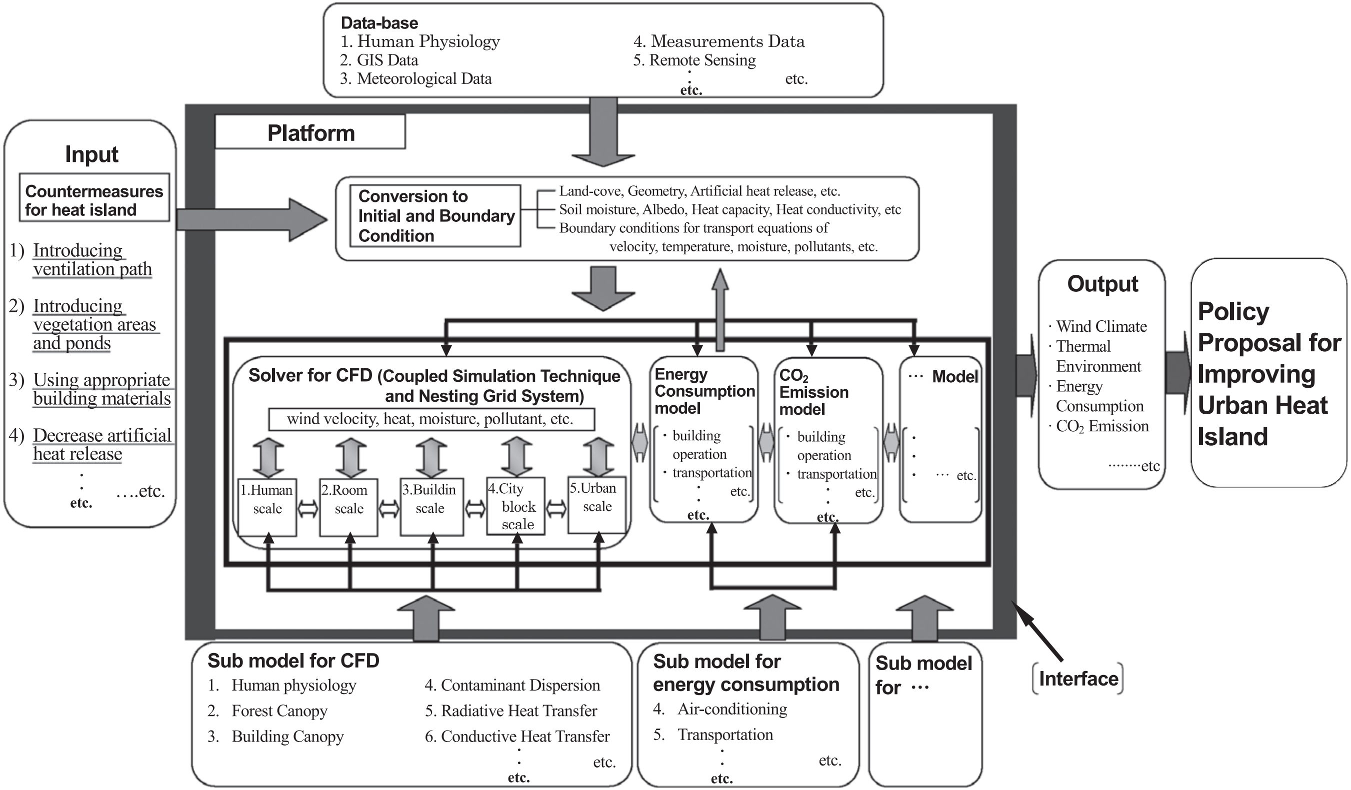


Fig. 14. Prototype of software platform for the total analysis of urban climate (Murakami et al. 2000; Murakami, 2004).

occur in LES. However, computational cost prohibits utilization of LES in practical applications. In order to overcome this drawback, the adaptation of hybrid RANS/LES and DES (detached-eddy simulation) appears to be necessary.

The latter part of the paper described the recent and future trends of numerical modeling for predicting the wind and thermal environment, as well as turbulent diffusion processes in real urban space in presence of various small SGS flow obstacles. The conventional approach in numerical modeling is generally carried out based on static condition (i.e. stationary objects such as buildings). This approach may be erroneous when applied to real situations, where dynamic conditions exist, e.g. due to non-stationary objects such as automobiles. In recent years, canopy models for reproducing the aerodynamic and thermal effects of trees/buildings/automobiles have been developed and applied to various problems related to urban climate. This paper demonstrated some of the results regarding this subject. The research studies emphasized the significance of the effects of stationary and non-stationary objects (tree canopy and vehicle canopy, respectively) on turbulent flowfield within street canyons.

As indicated in Section 4 in this paper, the development of the total simulation system integrating the submodel for the phenomena with various scales makes it possible to carry out total analysis of urban climate which comprises of many elements and is affected by many interacting physical processes at various scales. CWE is now in the process of growing from a tool for analysis to a tool for environmental design. However, a lot of improvements and revisions are still required before the turbulent flow phenomena in urban areas can be accurately reproduced. Hence, fundamental research efforts to improve the prediction accuracy should be continued.

## Acknowledgments

This paper reviewed the recent progress in CWE applied to environmental problems. Many topics included in this report are the results of collaborations extended over years with Prof. S. Murakami (Keio University), Prof. Y. Tominaga (Niigata Institute of Technology), Prof. R. Ooka (IIS, University of Tokyo), Dr. S. Iizuka (National Institute of Resources and Environment), Prof. S. Yoshida (Fukui University), Dr. K. Kondo (Kajima Corporation), Dr. K. Sasaki (Shimizu corporation) and Dr. T. Shirasawa (Tokyo Polytechnic University). The authors are grateful for their valuable contributions.

## References

Abe, K., Kondoh, T., Nagano, Y., 1995. A new turbulence model for predicting fluid flow and heat transfer in separating and reattaching flows—II. Thermal field calculations. Int. J. Heat Mass Transfer 38 (8), 1467–1481.

AIAA, 1998. Guide for the verification and validation of computational fluid dynamics simulations. AIAA G-077-1998.

Akabari, A., Davis, S., Dorsano, S., Huang, J., Winnett, S. (Eds.), 1992. Cooling Our Communities: A Guidebook to Tree Planting and Light Colored Surfacing. US EPA, Washington, DC.

Bardina, J., Ferziger, J.H., Reynolds, W.C., 1981. Improved subgrid-scale models for Large-Eddy Simulation. AIAA paper-80.

Blocken, B., Roels, S., Carmeliet, J., 2003. Pedestrian wind conditions in passages through buildings—Part 1. Numerical modeling, sensitivity analysis and experimental verification. Research Report, Laboratory of Building Physics, Catholic University of Leuven, 99pp.

Craft, T.J., Launder, B.E., 1992. A new model of 'Wall-Reflection' effects on the pressure–strain correlation and its application to the turbulent impinging jet. AIAA J. 30, 2970.

Craft, T.J., Launder, B.E., Suga, K., 1995. A non-liner eddy viscosity model including sensitivity to stress anisotropy. In: Proceedings of the 10th Symposium on Turbulent Shear Flows, Penn State University, 23/19–23/24.

Durbin, P.A., 1996. On the $k$–$\varepsilon$ stagnation point anomaly. Int. J. Heat Fluid Flow 17, 89–90.

ERCOFTAC, 2000. Best practices guidelines for industrial computational fluid dynamics, Version 1.0, January.

Ferziger, J.H., 1996. Large eddy simulation. In: Gatski, T.B., Hussain, M.Y., Lumley, J.L. (Eds.), Simulation and Modeling of Turbulent Flows. Oxford University Press, USA.

Franke, J., 2006. Recommendations of the COST action C14 on the use of CFD in predicting pedestrian wind environment. In: Proceedings of the Fourth International Symposium on Computational Wind Engineering (CWE2006), Yokohama, Japan, July 16–19, pp. 529–532.

Franke, J., Hirsch, C., Jensen, A.G., Krüs, H.W., Schatzmann, M., Westbury, P.S., Miles, S.D., Wisse, J.A., Wright, N.G., 2004. Recommendations on the use of CFD in wind engineering. In: Proceedings of the International Conference on Urban Wind Engineering and Building Aerodynamics. In: van Beeck, J.P.A.J. (Ed.), COST Action C14, Impact of Wind and Storm on City Life Built Environment. von Karman Institute, Sint-Genesius-Rode, Belgium, 5–7 May 2004.

Fu, S., Launder, B.E., Tselepidakis, D.P., 1987. Accommodating the effects of high strain rates in modeling the pressure–strain correlation. UMIST Mech. Eng. Dept. Rep., TFD/87/5.

Germano, M., Piomelli, U., Moin, P., Cabot, W.H., 1991. A dynamic subgrid scale eddy viscosity model. Phys. Fluids A 3 (7), 1760–1765.

Gibson, M.M., Launder, B.E., 1978. Ground effects on pressure fluctuations in the atmospheric boundary layer. J. Fluid Mech., 491–511.

Green, S.R., 1992. Modelling turbulent air flow in a stand of widely-spaced trees. PHOENICS J. Comput. Fluid Dyn. Appl. 5, 294–312.

Hanjalic, K., Kenjers, S., 2006. Some developments in turbulence modeling of environmental flows. In: Proceedings of The Fourth International Symposium on Computational Wind Engineering (CWE2006), Yokohama, Japan, July 16–19, pp. 65–94.

Hanjalic, K., Obi, S. (Eds.), 1997. Proceedings of the 6th ERCOFTAC/IAHR/COST Workshop on Refined Flow Modeling. Delft University of Technology.

Hataya, N., Mochida, A., Iwata, T., Tabata, Y., Yoshino, H., Tominaga, Y., 2006. Development of the simulation method for thermal environment and pollutant diffusion in street canyons with subgrid scale obstacles. In: Proceedings of the Fourth International Symposium on Computational Wind Engineering (CWE2006), Yokohama, Japan, July 16–19, pp. 553–556.

Hiraoka, H., 1993. Modelling of turbulent flows within plant/urban canopies. J. Wind Eng. Ind. Aerodyn. 46 & 47, 173–182.

Hiraoka, H., 2004. Modeling a microclimate within vegetation. NATO Advanced Study Institute—Flow and Transport Processes in Complex Obstructed Geometries from Cities and Vegetative Canopies to Industrial Problems. Kyiv, Ukraine, May 4–15, pp. 106–107.

Hiraoka, H., Ohashi, M., 2006. A ($k$–$\varepsilon$) turbulence closure model for plant canopy flows. In: Proceedings of the Fourth International Symposium on Computational Wind Engineering (CWE2006), Yokohama, Japan, July 16–19, pp. 693–696.

Iizuka, S., Kondo, H., 2004. Performance of various sub-grid scale models in large-eddy simulation of turbulent flow over complex terrain. Atmos. Environ. 38, 7083–7091.

Iizuka, S., Kondo, H., 2006. Large-eddy simulations of turbulent flow over complex terrain using modified static eddy viscosity models. Atmos. Environ. 40, 925–935.

Iizuka, S., Murakami, S., Tsuchiya, N., Mochida, A., 1999. LES of flow past 2D cylinder with imposed inflow turbulence. In: Proceedings of the 10th International Conference on Wind Engineering, Copenhagen, Denmark, vol. 2, pp. 1291–1298.

Inagaki, M., Kondoh, T., Nagano, Y., 2005. A mixed-time-scale SGS model with fixed model-parameters for practical LES. Trans. Am. Soc. Mech. Eng. J. Fluids Eng. 127, 1–13.

Kataoka, H., Mizuno, M., 2002. Numerical flow computation around aeroelastic 3D square cylinder using inflow turbulence. Wind Struct. 5 (2–4), 379–392.

Kenjers, S., Hanjalic, K., 2005. Dynamical simulations towards optimal indoor climate and safety control. In: CD Proceedings of the Third Dubrovnik Conference on Sustainable Development of Energy, Water and Environment System, Dubrovnik, Croatia, June 2005.

Kondo, K., Murakami, S., Mochida, A., 1997. Generation of velocity fluctuations for inflow boundary condition of LES. J. Wind Eng. Ind. Aerodyn. 67 & 68, 51–64.

Kondo, H., Tokairin, T., Kikegawa, Y., 2006. The wind calculation in Tokyo urban area with a mesoscale model. In: Proceedings of the Fourth International Symposium on Computational Wind Engineering (CWE2006), Yokohama, Japan, July 16–19, pp. 235–238.

Lakehal, D., Rodi, W., 1997. Calculation of the flow past a surface-mounted cube with two-layer turbulence models. J. Wind Eng. Ind. Aerodyn. 67 & 68, 65–78.

Launder, B.E., 1988. On the computation of convective heat transfer in complex turbulent flows. Trans. ASME J. Heat Transfer 110, 112–128.

Launder, B.E., Kato, M., 1993. Modeling flow-induced oscillations in turbulent flow around a square cylinder. In: ASME Fluid Engineering Conference.

Launder, B.E., Reece, G.J., Rodi, W., 1975. Progress in the development of a Reynolds-stress turbulence closure. J. Fluid Mech. 68, 537–566.

Lee, S., Lele, S.K., Moin, P., 1992. Simulation of spatially evolving turbulence and the applicability of Taylor's hypothesis in compressible flow. Phys. Fluids A 4 (7), 1521–1530.

Lilly, D.K., 1992. A proposed modification of the Germano subgrid-scale closure method. Phys. Fluids A 4 (3), 633–635.

Lin, B., Zhu, Y., Li, X., Qin, Y., 2006. Numerical simulation studies of the different vegetation patterns' effects on outdoor pedestrian comfort. In: Proceedings of the Fourth International Symposium on Computational Wind Engineering (CWE2006), Yokohama, Japan, July 16–19, pp. 521–524.

Liu, J., Chen, J.M., Black, T.A., Novak, M.D., 1996. $E$–$\varepsilon$ modelling of turbulent air flow downwind of a model forest edge. Boundary-Layer Meteorol. 77, 21–44.

Lun, Y.F., Mochida, A., Murakami, S., Yoshino, H., Shirasawa, T., 2003. Numerical simulation of flow over topographic features by revised $k$–$\varepsilon$ model. J. Wind Eng. Ind. Aerodyn. 91, 231–245.

Lund, T.S., Wu, X., Squires, K.D., 1998. Generation of turbulent inflow data for spatially-developing boundary layer simulations. J. Comput. Phys. 140, 233–2588.

Maruyama, T., 1993. Optimization of roughness parameters for staggered arrayed cubic blocks using experimental data. J. Wind Eng. Ind. Aerodyn. 46 & 47, 165–171.

Maruyama, T., Rodi, W., Maruyama, Y., Hiraoka, H., 1997. LES simulation of the turbulent boundary layer behind roughness elements using an artificially generated inflow. In: The Fourth Asia-Pacific Symposium on Wind Engineering, Volume of Abstract, pp. 371–374.

McPherson, E.G., Rowntree, R.A., 1993. Energy conservation potential of urban tree planting. J. Arboric. 19 (6), 321–331.

Meneveau, C., Lund, T.S., Cabot, W.H., 1996. A Lagrangian dynamic subgrid-scale model of turbulence. J. Fluid Mech. 319, 353–385.

Menter, F.R., Kunts, M., 2001. Development and applications of a zonal DES turbulence model for CFX-5. ANSYS CFX Validation Report, CFX-VAL 17/0703, pp. 1–34.

Mochida, A., 2005. Management and design of outdoor environment based on software platform for the total analysis of Urban Heat Island. In: CD Proceedings of the Third Dubrovnik Conference on Sustainable Development of Energy, Water and Environment System, Dubrovnik, Croatia, June 2005.

Mochida, A., Murakami, S., Ojima, T., Kim, S., Ooka, R., Sugiyama, H., 1997. CFD analysis of mesoscale climate in the Greater Tokyo area. J. Wind Eng. Ind. Aerodyn. 67 & 68, 459–477.

Mochida, A., Tominaga, Y., Murakami, S., Yoshie, R., Ishihara, T., Ooka, R., 2002. Comparison of various $k$–$\varepsilon$ models and DSM applied to flow around a high-rise building-report on AIJ cooperative project for CFD prediction of wind environment. Wind Struct. 5 (2–4), 227–244.

Mochida, A., Iwata, T., Hataya, N., Yoshino, H., Sasaki, K., Watanabe, H., 2005. Field measurements and CFD analyses of thermal environment and pollutant diffusion in street canyon. In: Proceedings of the Sixth Asia-Pacific Conference on Wind Engineering (APCWE-VI), pp. 2681–2696.

Mochida, A., Hataya, N., Iwata, T., Tabata, Y., Yoshino, H., Watanabe, H., 2006a. CFD analyses on outdoor thermal environment and air pollutant diffusion in street canyons under the influences of moving automobiles. In: Proceedings of the Sixth International Conference on Urban Climate (ICUC6), Goteborg, Sweden, June 12–16.

Mochida, A., Yoshino, H., Iwata, T., Tabata, Y., 2006b. Optimization of tree canopy model for CFD prediction of wind environment at pedestrian level. In: Proceedings of the Fourth International Symposium on Computational Wind Engineering (CWE2006), Yokohama, Japan, July 16–19, pp. 561–564.

Murakami, S., 2004. Indoor/outdoor climate design by CFD based on the software platform. Int. J. Heat Fluid Flow 25, 849–863.

Murakami, S., Mochida, A., 1999. Past, present, and future of CWE: the view from 1999. In: Larsen, A., Larose, G.L., Livesey, F.M. (Eds.), Wind Engineering into the 21st Century. Proceedings of 10th International Conference on Wind Engineering, Copenhagen, Denmark. A.A. Balkema, Rotterdam, pp. 91–104.

Murakami, S., Mochida, A., Hayashi, Y., 1990. Examining the $k$–$\varepsilon$ model by means of a wind tunnel test and large-eddy simulation of the turbulence structure around a cube. J. Wind Eng. Ind. Aerodyn. 35, 87–100.

Murakami, S., Mochida, A., Hayashi, Y., 1991. Scrutinizing $k$–$\varepsilon$ EVM and ASM by means of LES and wind tunnel for flowfield around cube. In: Preparation of the Eighth Symposium on Turbulent Shear Flows, Munich, Germany, pp. 17-1-1–17-1-6.

Murakami, S., Mochida, A., Ooka, R., 1993. Numerical simulation of flowfield over surface-mounted cube with various second-moment closure models. In: Preparation of the Ninth Symposium on Turbulent Shear Flows. Kyoto, Japan, pp. 13-5-1–13-5-6.

Murakami, S., Iizuka, S., Mochida, A., Tominaga, Y., 1996a. LES analysis of turbulent flow past a square cylinder using various SGS models. In: Chollet, J.P., Voke, P.R., Kleiser, L. (Eds.), Second ERCORTAC Workshop: Direct and Large-eddy Simulation II, Grenoble, France, pp. 385–395.

Murakami, S., Mochida, A., Iizuka, S., 1996b. New trends in turbulence models for prediction of wind effects on structures. In: IWEF Workshop on CWE/CFD for Prediction of Wind Effects on Structures, pp. 1–52.

Murakami, S., Ooka, R., Iizuka, S., 1999. CFD analysis of flow past two-dimensional square cylinder using dynamic LES. J. Fluids Struct. 13, 1097–1112.

Murakami, S., Mochida, A., Kim, S., Ooka, R., Yoshida, S., Kondo, H., Genchi, Y., Shimada, A., 2000. Software platform for the total analysis of wind climate and urban heat island. In: Proceedings of the Third International Symposium on Computational Wind Engineering, pp. 23–26.

Murakami, S., Mochida, A., Kato, S., 2003a. Development of local area wind prediction system for selecting suitable site for windmill. J. Wind Eng. Ind. Aerodyn. 91, 1759–1776.

Murakami, S., Mochida, A., Ooka, R., Yoshida, S., Yoshino, H., Sasaki, K., Harayama, K., 2003b. Evaluation of the impacts of urban tree planting in Tokyo based on Urban Heat Balance model. In: Conference Preprints of the 11th International Conference on Wind Engineering, vol. 2, pp. 2641–2648.

Murakami, S., Otsuka, K., Mochida, A., Kataoka, H., Kato, S., 2003c. CFD prediction of flow over complex terrain using Local Area Wind Energy Prediction System (LAWEPS). In: Conference Preprints of the 11th International Conference on Wind Engineering, Texas, vol. 2, pp. 2821–2828.

Nagano, Y., Hattori, H., 2003. A new low-Reynolds number turbulence model with hybrid time-scale of mean flow and turbulence for complex wall flow. In: Hanjalic, K., Nagano, Y., Arinc, F. (Eds.), Proceedings of the Fourth International Symposium on Turbulence, Heat and Mass Transfer, Antalya, Turkey.

Ohashi, M., 2004. A study on analysis of airflow around an individual tree. J. Environ. Eng., AIJ No.578, April, 91–96. (in Japanese).

Omori, T., Taniguchi, H., Kudo, K., 1990. Monte-Carlo simulation of indoor radiant environment. Int. J. Numer. Methods Eng 30 (4), 615–627.

Ooka, R., Harayama, K., Murakami, S., Kondo, H., 2004. In: Fifth Symposium on the Urban Environment, Annual Meeting of American Meteorological Society, Vancouver, British Columbia, Canada, pp. 9–15.

Ooka, R., Chen, H., Kato, S., 2006. Study on optimum arrangement of trees for design of pleasant outdoor environment using multi-objective genetic algorithm. In: Proceedings of the Fourth International Symposium on Computational Wind Engineering (CWE2006), Yokohama, Japan, July 16–19, pp. 525–528.

Richards, P.J., Mallinson, G.D., McMillan, D., Li, Y.F., 2002. Pedestrian level wind speeds in downtown Auckland. Wind Struct. 5 (2–4), 151–164.

Roache, P.J., Ghia, K., White, F. (Eds.), 1986. Editorial policy statement on the control of numerical accuracy, ASME J. Fluids Eng. 108 (1), 2.

Rodi, W., 1976. A new algebraic relation for calculating the Reynolds stresses. ZAMM 56, T219–T221.

Rodi, W., 1997. Comparison of LES and RANS calculations of the flow around bluff bodies. J. Wind. Eng. Ind. Aerodyn. 69–71, 55–75.

Rodi, W., Ferziger, J.H., Breuer, M., Pourquie, M., 1997. Status of large eddy simulation: results of workshop. Trans. ASME J. Fluids Eng. 119, 248–262.

Rowntree, R.A., 1989. Ecological values of the urban forest. In: Proceedings of the Fourth Urban Forestry Conference. American Forestry Association, Washington, DC, pp. 22–25.

Sasaki, K., Mochida, A., Yoshida, T., Yoshino, H., Watanabe, H., 2006. A new method to select appropriate countermeasures against heat-island effects according to the regional characteristics of heat balance mechanism. In: Proceedings of the Fourth International Symposium on Computational Wind Engineering (CWE2006), Yokohama, Japan, July 16–19, pp. 223–226.

Sato, T., Murakami, S., Ooka, R., Yoshida, S., 2006. Analysis of regional characteristics of the atmospheric heat balance in the Tokyo metropolitan area in summer. In: Proceedings of the Fourth International Symposium on Computational Wind Engineering (CWE2006), Yokohama, Japan, July 16–19, pp. 231–234.

Shih, T.H., Zhu, J., Lumley, J.L., 1993. A realizable Reynolds stress algebraic equation model. NASA report, TM-105993.

Shirasawa, T., Mochida, A., Tominaga, Y., Yoshino, H., 2006. Evaluation of turbulent time scale of linear revised $k$–$\varepsilon$ model based on LES data. In: Proceedings of the Fourth International Symposium on Computational Wind Engineering (CWE2006), Yokohama, Japan, July 16–19, pp. 125–128.

Spalart, P.R., 1999. Strategies for Turbulence Modelling and Simulations, Engineering Turbulence Modelling and Experiments-4. Elsevier Science Ltd., Amsterdam, pp. 3–17.

Speziale, C.G., 1987. On nonlinear $k$–$l$ and $k$–$\varepsilon$ models of turbulence. J. Fluid Mech. 178, 459–475.

Speziale, C.G., Sarkar, S., Gatski, T.B., 1991. Modeling the pressure–strain correlation of turbulence: an invariant dynamical system approach. J. Fluid Mech. 227, 245–272.

Squires, K.D., 2003. Perspective and challenges in simulation and modeling of unsteady flows. In: CD Proceedings of the 17th Japan National Conference on Computational Fluid Dynamics.

Squires, K.D., 2006. Prediction of turbulent flows at high Reynolds numbers using detached-eddy simulation. In: Proceedings of the Fourth International Symposium on Computational Wind Engineering (CWE2006), Yokohama, Japan, July 16–19, pp. 61–64.

Stathopoulos, T., Baskaran, A., 1996. Computer simulation of wind environmental conditions around buildings. Eng. Struct. 18 (11), 876–885.

Svensson, U., Häggkvist, K., 1990. A two-equation turbulence model for canopy flows. J. Wind Eng. Ind. Aerodyn. 35, 201–211.

Timofeyef, N., 1998. Numerical study of wind mode of a territory development. In: Proceedings of the Second East European Conference on Wind Engineering, September 7–11, Prague, Czech Republic.

Tominaga, Y., Mochida, A., 1999. CFD prediction of flowfield and snowdrift around building complex in snowy region. J. Wind Eng. Ind. Aerodyn. 81, 272–282.

Tominaga, Y., Murakami, S., Mochida, A., 1997. CFD prediction of gaseous diffusion around a cubic model using a dynamic mixed SGS model based on composite grid technique. J. Wind Eng. Ind. Aerodyn. 67 & 68, 827–841.

Tominaga, Y., Mochida, A., Murakami, S., 2003. Large eddy simulation of flowfield around a high-rise building. In: Conference Preprints of the 11th International Conference on Wind Engineering, vol. 2, pp. 2543–2550.

Tominaga, Y., Mochida, A., Shirasawa, T., Yoshie, R., Kataoka, H., Harimoto, K., Nozu, T., 2004. Cross comparisons of CFD results of wind environment at Pedestrian level around a high-rise building and within a building complex. J. Asian Archit. Build. Eng. 3 (1), 63–70.

Tominaga, Y., Yoshie, R., Mochida, A., Kataoka, H., Harimoto, K., Nozu, T., 2005. Cross comparison of CFD prediction for wind environment at pedestrian level around buildings (Part 2). In: Proceedings of the Sixth Asia-Pacific Conference on Wind Engineering (APCWE-VI), pp. 2661–2670.

Tominaga, Y., Mochida, A., Yoshie, R., 2006. AIJ guideline for practical applications of CFD to wind environment around buildings. In: Proceedings of the Fourth International Symposium on Computational Wind Engineering (CWE2006), Yokohama, Japan, July 16–19, pp. 533–536.

Tsuchiya, M., Murakami, S., Mochida, A., Kondo, K., Ishida, Y., 1997. Development of new $k$–$\varepsilon$ model for flow and pressure fields around bluff body. J. Wind. Eng. Ind. Aerodyn. 67 & 68, 169–182.

Uno, I., Ueda, H., Wakamatsu, S., 1989. Numerical modeling of the nocturnal urban boundary layer. Boundary-Layer Meteorol. 49, 77–98.

Voke, P.R., 1996. Flow past a square cylinder: test case LES2. In: Chollet, J.P., Voke, P.R., Kleiser, L. (Eds.), Second ERCORTAC Workshop: Direct and Large-eddy Simulation II, Gronouble, France.

Vreman, B., Geurts, B., Kuerten, H., 1994. On the formulation of the dynamic mixed subgrid-scale model. Phys. Fluids A 6, 4057.

Watanabe, H., Mochida, A., Sakaida, K., Yoshino, H., Jyu-nimura, Y., Iwata, T., Hataya, N., Shibata, K., 2005. Field measurement of thermal environment and pollutant diffusion in street canyon to investigate the effects of its form and roadside trees. In: Proceedings of International Symposium on Sustainable Development of Asia City Environment (SDACE 2005). Department of Architecture, Xi'an, China, November 23–25, pp. 509–515.

Westbury, P.S., Miles, S.D., Stathopoulos, T., 2002. CFD application on the evaluation of pedestrian-level winds. In: Workshop on Impact of Wind and Storm on City Life and Built Environment, Cost Action C14, CSTB, June 3–4, Nantes, France.

World Urbanization Prospects: The 2001 Revision. Department of Economic and Social Affairs Population Division, UN (www.un.org/esa/population/publications/wup2001/WUP2001_CH1.pdf).

Wright, N.G., Easom, G.J., 1999. Comparison of several computational turbulence models with full-scale measurements of flow around a building. Wind Struct. 2 (4).

Wright, N.G., Easom, G.J., Hoxey, R.J., 2001. Development and validation of a non-linear $k$–$\varepsilon$ model for flow over a full-scale building. Wind Struct. 4 (3).

Yakhot, V., Orsag, S.A., 1986. Renormalization group analysis of turbulence. J. Sci. Comput. 1, 3.

Yamada, T., 1982. A numerical model study of turbulent airflow in and above a forest canopy. J. Meteorol. Soc. Jpn. 60 (1), 439–454.

Yang, W., Jin, S., Xinyang, S., Jin, H., Quan, Y., Gu, M., 2006. Research on the parameters of turbulence model and modeling of equilibrium atmosphere boundary layer in CWE. In: Proceedings of the Fourth International Symposium on Computational Wind Engineering (CWE2006), Yokohama, Japan, July 16–19, pp. 901–904.

Yoshida, S., Murakami, S., Ooka, R., Mochida, A., Tominaga, Y., 2000. Influence of green area ratio on outdoor of convection, radiation and moisture transport. Comput. Wind Eng. 2000, 27–30.

Yoshida, S., Ooka, R., Mochida, A., Murakami, S., Tominaga, Y., 2006. Development of three dimensional plant canopy model for numerical simulation of outdoor thermal environment. In: Proceedings of the Sixth International Conference on Urban Climate (ICUC 6), Goteborg, Sweden, June 12–16.

Yoshie, R., Mochida, A., Tominaga, Y., Kataoka, H., Harimoto, K., Nozu, T., Shirasawa, T., 2005a. Cooperative project for CFD prediction of pedestrian wind environment in the Architectural Institute of Japan. In: CD Proceedings of EACWE4—the Fourth European and African Conference on Wind Engineering, Paper no. 292.

Yoshie, R., Mochida, A., Tominaga, Y., Kataoka, H., Yoshikawa, M., 2005b. Cross comparison of CFD prediction for wind environment at pedestrian level around buildings (Part 1). In: Proceedings of the Sixth Asia-Pacific Conference on Wind Engineering (APCWE-VI), pp. 2648–2660.

Yoshie, R., Mochida, A., Tominaga, Y., 2006. CFD prediction of wind environment around a high-rise building located in an urban area. In: Proceedings of the Fourth International Symposium on Computational Wind Engineering (CWE2006), Yokohama, Japan, July 16–19, pp. 129–132.

Zang, Y., Street, R.L., Koseff, J.R., 1993. A dynamic mixed subgrid scale model and its application to turbulent recirculating flows. Phys. Fluids A 5 (12).